[54] A. Nanda, R. Romanek, J.T. Curnutte, S. Grinstein, Assessment of the contribution of the cytochrome *b* moiety of the NADPH oxidase to the transmembrane H^+ conductance of leukocytes, J. Biol. Chem. 269 (1994) 27280–27285.
[55] Y.F. Hui, S.Y. Chan, Y.L. Lau, Identification of mutations in seven Chinese patients with X-linked chronic granulomatous disease, Blood 88 (1996) 4021–4028.
[56] M. Jurkowska, M. Kurenko-Deptuch, J. Bal, D. Roos, The search for a genetic defect in Polish patients with chronic granulomatous disease, Arch. Immunol. Ther. Exp. (Warsz.) 52 (2004) 441–446.
[57] H. Khaldi, S. Marchand-Adam, C. Kannengiesser, A. Fabre, M.P. Debray, C. Danel, M.A. Gougerot-Pocidalo, J. El Benna, M. Humbert, M. Aubier, B. Crestani, Eur. Respir. J. 33 (2009) 1498–1502.
[58] J. Brunner, G. Dockter, A. Rösen-Wolff, J. Roesler, X-linked chronic granulomatous disease (CGD) caused by an intra-exonic splice mutation (*CYBB* exon 3, c.262G→A) is mimicking juvenile sarcoidosis, Clin. Exp. Rheumatol. 25 (2007) 336–338.
[59] E.M. Lewis, M. Singla, S. Sergeant, P.P. Koty, L.C. McPhail, X-linked chronic granulomatous disease secondary to skewed X chromosome inactivation in a female with a novel CYBB mutation and late presentation, Clin. Immunol. 129 (2008) 372–380.
[60] B. Brouha, C. Meischl, E. Ostertag, M. de Boer, Y. Zhang, H. Neijens, D. Roos, H.H. Kazazian Jr., Evidence consistent with human L1 retrotransposition in maternal meiosis I, Am. J. Hum. Genet. 71 (2002) 327–336.
[61] P.J. Patiño, J.E. Perez, J.A. Lopez, A. Condino-Neto, A.S. Grumach, J.H. Botero, J.T. Curnutte, D. García de Olarte, Molecular analysis of chronic granulomatous disease caused by defects in gp91-*phox*, Hum. Mutat. 13 (1999) 29–37.
[62] P. Vilaiphan, P. Chatchatee, J. Ngamphaiboon, S. Tongkobpetch, K. Suphapeetiporn, V. Shotelersuk, Nonsense mutations of the *CYBB* gene in two Thai families with X-linked chronic granulomatous disease, Asian Pac. J. Allergy Immunol. 25 (2007) 243–247.
[63] M. Tsuda, M. Kaneda, T. Sakiyama, I. Inana, M. Owada, C. Kiryu, T. Shiraishi, K. Kakinuma, A novel mutation at a probable heme-binding ligand in neutrophil cytochrome b_{558} in atypical X-linked chronic granulomatous disease, Hum. Genet. 103 (1998) 377–381.
[64] M. Kaneda, H. Sakubara, A. Ohtake, A. Nishida, C. Kiryu, K. Kakinuma, Missense mutations in the $gp91^{phox}$ gene encoding cytochrome b_{558} in patients with cytochrome *b* positive and negative X-linked chronic granulomatous disease, Blood 93 (1999) 2098–2104.
[65] S. Chollet-Martin, A. Lopez, C. Gaud, D. Henry, B. Stos, J. El Benna, G. Chedevile, D. Gendrel, M.A. Gougerot-Pocidalo, B. Grandchamp, B. Gérard, Severe X-linked chronic granulomatous disease in two unrelated females, Eur. J. Pediatr. 166 (2007) 153–159.
[66] A. Lun, J. Roesler, H. Renz, Unusual late onset of X-linked chronic granulomatous disease in an adult woman after unsuspicious childhood, Clin. Chem. 48 (2002) 780–781.
[67] T. Ariga, Y. Sakiyama, H. Furuta, S. Matsumoto, Molecular genetic studies of two families with X-linked chronic granulomatous disease: mutation analysis and definitive determination of carrier status in patient's sisters, Eur. J. Haematol. 52 (1994) 99–102.
[68] D. Noack, P.G. Heyworth, P.E. Newburger, A.R. Cross, An unusual intronic mutation in the *CYBB* gene giving rise to chronic granulomatous disease, Biochim. Biophys. Acta 1537 (2001) 125–131.
[69] J. Bustamante, G. Aksu, G. Vogt, L. de Beaucoudrey, F. Genel, A. Chapgier, O. Filipe-Santos, J. Feinberg, J.F. Emile, N. Kutukculer, J.L. Casanova, BCG-osis and tuberculosis in a child with chronic granulomatous disease, J. Allergy Clin. Immunol. 120 (2007) 32–38.
[70] C. Meischl, M. de Boer, A. Åhlin, D. Roos, A new exon created by intronic insertion of a rearranged LINE-1 element as the cause of chronic granulomatous disease, Eur. J. Hum. Genet. 8 (2000) 697–703.
[71] V. Jendrossek, A. Ritzel, B. Neubauer, S. Heyden, M. Gahr, An in-frame triplet deletion within the gp91-*phox* gene in an adult X-linked chronic granulomatous disease patient with residual NADPH-oxidase activity, Eur. J. Haematol. 58 (1997) 78–85.
[72] M. Yamada, Y. Suzuki, S. Fukumura, T. Miyazaki, H. Ikeda, Y. Okura, S. Takezaki, N. Kawamura, T. Ariga, Somatic mosaicism detected in two patients with X-linked chronic granulomatous disease, Clin. Exp. Immunol. 154 (Suppl. 1) (2008) 153.
[73] A. Rump, A. Rösen-Wolff, M. Gahr, J. Seidenberg, C. Roos, L. Walter, V. Günther, J. Roesler, A splice-supporting intronic mutation in the last bp position of a cryptic exon within intron 6 of the *CYBB* gene induces its incorporation into the mRNA causing chronic granulomatous disease (CGD), Gene 371 (2006) 174–181.
[74] D. Noack, P.G. Heyworth, J.T. Curnutte, J. Rae, A.R. Cross, A novel mutation in the *CYBB* gene resulting in an unexpected pattern of exon skipping and chronic granulomatous disease, Biochim. Biophys. Acta 1454 (1999) 270–274.
[75] H. Rabbani, M. De Boer, A. Åhlin, U. Sundin, G. Elinder, L. Hammarström, J. Palmblad, C.I. Smith, D. Roos, A 40-base-pair duplication in the gp91-*phox* gene leading to X-linked chronic granulomatous disease, Eur. J. Haematol. 51 (1993) 218–222.
[76] J.T. Curnutte, P.J. Hopkins, W. Kuhl, E. Beutler, Studying X inactivation, Lancet 339 (1992) 749.
[77] W.I. Lee, T.H. Jaing, M.Y. Hsieh, M.L. Kuo, S.J. Lin, J.L. Huang, Distribution, infections, treatments and molecular analysis in a large cohort of patients with primary immunodeficiency diseases (PIDs) in Taiwan, J. Clin. Immunol. 26 (2006) 274–283.
[78] M.Y. Köker, O. Sanal, M. De Boer, I. Tezcan, A. Metin, F. Ersoy, D. Roos, Mutations of chronic granulomatous disease in Turkish families, Eur. J. Clin. Invest. 37 (2007) 589–595.
[79] H.N. Bu-Ghanim, A.W. Segal, N.H. Keep, C.M. Casimir, Molecular analysis in three cases of $X91^-$ variant chronic granulomatous disease, Blood 86 (1995) 3575–3582.
[80] S.J. Lin, Y.F. Huang, J.Y. Chen, P.G. Heyworth, D. Noack, J.Y. Wang, C.Y. Lin, B.L. Chiang, C.M. Yang, C.C. Liu, C.C. Shieh, Molecular quality control machinery contributes to the leukocyte NADPH oxidase deficiency in chronic granulomatous disease, Biochim. Biophys. Acta 1586 (2002) 275–286.
[81] M. Anderson-Cohen, S.M. Holland, D.B. Kuhns, T.A. Fleisher, L. Ding, S. Brenner, H.L. Malech, J. Roesler, Severe phenotype of chronic granulomatous disease presenting in a female with a de novo mutation in gp91-*phox* and a non familial, extremely skewed X chromosome inactivation, Clin. Immunol. 109 (2003) 308–317.
[82] A. Rösen-Wolff, W. Soldan, K. Heyne, J. Bickhardt, M. Gahr, J. Roesler, Increased susceptibility of a carrier of X-linked chronic granulomatous disease (CGD) to Aspergillus fumigatus infection associated with age-related skewing of lyonization, Ann. Hematol. 80 (2001) 113–115.
[83] M.J. Stasia, B. Lardy, A. Maturana, P. Rousseau, C. Martel, P. Bordigoni, N. Demaurex, F. Morel, Molecular and functional characterization of a new X-linked chronic granulomatous disease variant ($X91^+$) case with a double missense mutation in the cytosolic gp91-*phox* C-terminal tail, Biochim. Biophys. Acta 1586 (2002) 316–330.
[84] C. Bionda, X.J. Li, R. van Bruggen, M. Eppink, D. Roos, F. Morel, M.J. Stasia, Functional analysis of two-amino acid substitutions in gp91-*phox* in a patient with X-linked flavocytochrome b_{558}-positive chronic granulomatous disease by means of transgenic PLB-985 cells, Hum. Genet. 115 (2004) 418–427.
[85] L.S. Yoshida, F. Saruta, K. Yoshikawa, O. Tatsuzawa, S. Tsunawaki, Mutation at histidine 338 of $gp91^{phox}$ depletes FAD and affects expression of cytochrome b_{558} of the human NADPH oxidase, J. Biol. Chem. 273 (1998) 27879–27886.
[86] T. Ariga, Y. Sakiyama, S. Matsumoto, Two novel point mutations in the cytochrome b_{558} heavy chain gene, detected in two Japanese patients with X-linked chronic granulomatous disease, Hum. Genet. 94 (1994) 441.
[87] B. Wolach, S. Ash, R. Gavrieli, B. Stark, I. Yaniv, D. Roos, Acute lymphoblastic leukemia in a patient with chronic granulomatous disease and a novel mutation in *CYBB*: first report, Am. J. Hematol. 80 (2005) 50–54.
[88] J.H. Leusen, C. Meischl, M.H. Eppink, P.M. Hilarius, M. de Boer, R.S. Weening, A. Ahlin, L. Sanders, D. Goldblatt, H. Skopczynska, E. Bernatowska, J. Palmblad, A.J. Verhoeven, W.J. van Berkel, D. Roos, Four novel mutations in the gene encoding gp91-*phox* of human NADPH oxidase: consequences for oxidase assembly, Blood 95 (2000) 666–673.
[89] T. Ariga, Y. Sakiyama, S. Matsumoto, A 15-base pair (bp) palindromic insertion associated with a 3-bp deletion in exon 10 of the $gp91^{phox}$ gene, detected in two patients with X-linked chronic granulomatous disease, Hum. Genet. 96 (1995) 6–8.
[90] F.G. Bakri, C. Martel, N. Khuri-Bulos, A. Mahafzah, M.S. El-Khateeb, A.M. Al-Wahadneh, W.A. Hayajneh, H.A. Hamamy, E. Maquet, M. Molin, M.J. Stasia, First report of clinical, functional, and molecular investigation of chronic granulomatous disease in nine Jordanian families, J. Clin. Immunol. 29 (2009) 215–230.
[91] M.C. Dinauer, J.T. Curnutte, H. Rosen, S.H. Orkin, A missense mutation in the neutrophil cytochrome b heavy chain in cytochrome-positive X-linked chronic granulomatous disease, J. Clin. Invest. 84 (1989) 2012–2016.
[92] B.L. Schapiro, P.E. Newburger, M.S. Klempner, M.C. Dinauer, Chronic granulomatous disease presenting in a 69-year-old man, N. Engl. J. Med. 325 (1991) 1786–1790.
[93] J.H.W. Leusen, M. De Boer, B.G.J.M. Bolscher, P.M. Hilarius, R.S. Weening, H.D. Ochs, D. Roos, A.J. Verhoeven, A point mutation in $gp91^{phox}$ of cytochrome b_{558} of the human NADPH oxidase leading to defective translocation of the cytosolic proteins $p47^{phox}$ and $p67^{phox}$, J. Clin. Invest. 93 (1994) 2120–2126.
[94] H. Azuma, H. Oomi, K. Sasaki, I. Kawabata, T. Sakaino, S. Koyano, T. Suzutani, H. Nunoi, A. Okuno, A new mutation in exon 12 of the $gp91^{phox}$ gene leading to cytochrome *b*-positive X-linked chronic granulomatous disease, Blood 85 (1995) 3274–3277.
[95] O. Jirapongsananuruk, D. Noack, S. Boonchoo, C. Thepthai, K. Chokephaibulkit, N. Visitsunthorn, P. Vichyanond, V. Luangwedchakarn, S. Likasitwattanakul, S. Piboonpocanun, A novel mutation of the *CYBB* gene resulting in severe form of X-linked chronic granulomatous disease, Asian Pac. J. Allergy Immunol. 25 (2007) 249–252.
[96] J.P. DeMore, Y. Dong, D.B. Lewis, J.E. Gern, C.M. Seroogy, A novel missense mutation in *CYBB* gene in chronic granulomatous disease, J. Allergy Clin. Immunol. 119 (Suppl. 1) (2007) S257.
[97] S. Al-Muhsen, A. Al-Hemidan, A. Al-Shehri, A. Al-Harbi, A. Al-Ghonaium, B. Al-Saud, H. Al-Mousa, H. Al-Dhekri, R. Arnaout, I. Al-Mohsen, O. Alsmadi, Ocular manifestations in chronic granulomatous disease in Saudi Arabia, J. Am. Assoc. Pediatr. Ophthalmol. Strabismus 13 (2009) 396–399.
[98] S.C. Chien, C.N. Lee, C.C. Hung, P.N. Tsao, Y.N. Su, F.J. Hsieh, Rapid prenatal diagnosis of X-linked chronic granulomatous disease using a denaturing high-performance liquid chromatography (DHPLC) system, Prenat. Diagn. 23 (2003) 1092–1096.
[99] J. Peng, C.M. Redman, X. Wu, X. Song, R.H. Walker, C.M. Westhoff, S. Lee, Insights into extensive deletions around the *XK* locus associated with McLeod phenotype and characterization of two novel cases, Gene 392 (2007) 142–150.
[100] U. Francke, H.D. Ochs, B. de Martinville, J. Giacalone, V. Lindgren, C. Distèche, R.A. Pagon, M.H. Hofker, G.J. van Ommen, P.L. Pearson, R.J. Wedgwood, Minor Xp21 chromosome deletion in a male associated with expression of Duchenne muscular dystrophy, chronic granulomatous disease, retinitis pigmentosa, and McLeod syndrome, Am. J. Hum. Genet. 37 (1985) 250–267.
[101] B. Royer-Pokora, L.M. Kunkel, A.P. Monaco, S.C. Goff, P.E. Newburger, R.L. Baehner, F.S. Cole, J.T. Curnutte, S.H. Orkin, Cloning the gene for an inherited human disorder–chronic granulomatous disease–on the basis of its chromosomal location, Nature 322 (1986) 32–38.
[102] M.A. Deardorff, H. Gaddipati, P. Kaplan, P.A. Sanchez-Lara, N. Sondheimer, N.B. Spinner, H. Hakonarson, C. Ficicioglu, J. Ganesh, T. Markello, B. Loechelt, D.J. Zand, M. Yudkoff, U. Lichter-Konecki, Complex management of a patient with a contiguous

Xp11.4 gene deletion involving ornithine transcarbamylase: a role for detailed molecular analysis in complex presentations of classical diseases, Mol. Genet. Metab. 94 (2008) 498–502.
[103] D. Frey, M. Mächler, R. Seger, W. Schmid, S.H. Orkin, Gene deletion in a patient with chronic granulomatous disease and McLeod syndrome: fine mapping of the *Xk* gene locus, Blood 71 (1988) 252–255.
[104] Y. Okubo, T. Tanaka, K. Yoshikawa, K. Hattori, Y. Kobayashi, T. Seno, Y. Okubo, A male infant of X-linked chronic granulomatous disease associated with the McLeod red cell phenotype, J. Jpn. Pediatr. Soc. 96 (1992) 162–167.
[105] G. De Saint-Basile, M.C. Bohler, A. Fischer, J. Cartron, J.L. Dufier, C. Griscelli, S.H. Orkin, Xp21 DNA microdeletion in a patient with chronic granulomatous disease, retinitis pigmentosa, and Mcleod phenotype, Hum. Genet. 80 (1988) 85–89.
[106] N. Mahlaoui, M.D. Dumont, P.Y. Le Pennec, P. Frange, D. Moshous, P. Bierling, A. Fischer, Chronic granulomatous disease and McLeod syndrome: single center report of four cases, Clin. Exp. Immunol. 154 (Suppl. 1) (2008) 146.
[107] C. Schuetz, M. Hoenig, A. Schulz, M.A. Lee-Kirsch, J. Roesler, W. Friedrich, H. von Bernuth, Successful unrelated bone marrow transplantation in a child with chronic granulomatous disease complicated by pulmonary and cerebral granuloma formation, Eur. J. Pediatr. 166 (2007) 785–788.
[108] N.N. Faizunnessa, T. Tsuchiya, A. Kumatori, H. Kurozumi, S. Imajoh-Ohmi, S. Kanegasaki, M. Nakamura, A 25-kb deletion in the 5′ region of the cytochrome b_{558} heavy chain gene (*CYBB*) in a patient with X-linked chronic granulomatous disease, Hum. Genet. 99 (1997) 469–473.
[109] A. Kumatori, N.N. Faizunnessa, S. Suzuki, T. Moriuchi, H. Kurozumi, M. Nakamura, Nonhomologous recombination between the cytochrome b_{558} heavy chain gene (*CYBB*) and LINE-1 causes an X-linked chronic granulomatous disease, Genomics 53 (1998) 123–128.
[110] A. Pelham, M.A. O'Reilly, S. Malcolm, R.J. Levinsky, C. Kinnon, RFLP and deletion analysis for X-linked chronic granulomatous disease using the cDNA probe: potential for improved prenatal diagnosis and carrier determination, Blood 76 (1990) 820–824.
[111] M. de Boer, E. Bakker, S. Van Lierde, D. Roos, Somatic triple mosaicism in a carrier of X-linked chronic granulomatous disease, Blood 91 (1998) 252–257.
[112] Z. Rezvani, I. Mohammadzadeh, Z. Pourpak, M. Moin, S. Teimourian, *CYBB* gene mutation detection in an Iranian patient with chronic granulomatous disease, Iran. J. Allergy Asthma Immunol. 4 (2005) 103–106.
[113] F. Kuribayashi, M. de Boer, J.H. Leusen, A.J. Verhoeven, D. Roos, A novel polymorphism in the coding region of *CYBB*, the human gp91-*phox* gene, Hum. Genet. 97 (1996) 611–613.

TABLE 2 Details of response to sequential treatments where applicable ($n = 10$)

No.	Severity of disease	First treatment		Second treatment		Third treatment	
1	Severe	Amlodopine	×	Nifedipine	√	–	–
2	Moderate	Amlodopine	×	GTN	×	–	–
3	Moderate	Amlodopine	×	GTN	×	–	–
4	Severe	Nifedipine	×	Amlodopine	×	–	–
5	Severe	Nifedipine	×	Amlodopine	×	GTN	√
6	Moderate	Nifedipine	×	GTN	×	–	
7	Severe	GTN	×	Amlodopine	×	Nifedipine	√
8	Moderate	Nifedipine	×	GTN	√	–	–
9	Severe	Amlodopine	×	Nifedipine	×	GTN	×
10	Moderate	Amlodopine	√	GTN	√	–	–

×: no response/inadequate response; √: response.

Overall, GTN patches were effective in 55% of the treated patients. Efficacy was better than that of nifedipine and amlodipine (33 *vs* 25% response rate, respectively), but small numbers and retrospective analysis does not allow statistical comparison. Response was similar in primary and secondary RP. Children with severe RP had a better response to nifedipine and amlodopine than children with moderate disease. The sub-group with severe disease was more likely to be using a disease-modifying drug, which may have had an impact. However, numbers are too small for any conclusion to be drawn from this.

Application of GTN patches allows removal if adverse events occur. Together with absence of tablets, this may make treatment with GTN attractive in paediatric practice. All patients received Deponit GTN patches. Alternative brands may not have adequate skin adhesion when cut into quarters for this off-license use.

GTN patches, nifedipine and amlodipine offer symptomatic relief for patients with moderate primary/secondary RP. Further studies, including head-to-head trials, are needed to determine if one agent is superior. Meanwhile, GTN patches offer an alternative to oral calcium channel blockers for symptomatic relief of paediatric RP.

Rheumatology key message

- GTN patches are an efficacious treatment option in paediatric RP.

Disclosure statement: The authors have declared no conflicts of interest.

Kapil Gargh[1], Eileen M. Baildam[1], Gavin A. Cleary[1], Michael W. Beresford[1] and Liza J. McCann[1]

[1]*Department of Paediatric Rheumatology, Alder Hey Children's NHS Foundation Trust, Liverpool, UK*
Accepted 20 August 2009
Correspondence to: Liza McCann, Department of Paediatric Rheumatology, Alder Hey Children's NHS Foundation Trust, Eaton Road, Liverpool, L12 2AP, UK.
E-mail: liza.mccann@alderhey.nhs.uk

References

1 Anderson ME, Moore TL, Hollis S, Jayson MIV, King TA, Herrick AL. Digital vascular response to topical glyceryl trinitrate, as measured by laser Doppler imaging, in primary Raynaud's phenomenon and systemic sclerosis. Rheumatology 2002;41:324–28.

2 Franks AG Jr. Topical glyceryl trinitrate as adjunctive treatment in Raynaud's disease. Lancet 1982;1:76–7.

3 Teh LS, Mannig J, Moore T, Tully MP, O'Reilly D, Jayson MIV. Sustained-release transdermal glyceryl trinitrate patches as a treatment for primary and secondary Raynaud's phenomenon. Br J Rheumatol 1995; 34:636–41.

4 Nigrovic PA, Fuhlbrigge RC, Sundel RP. Raynaud's phenomenon in children: a retrospective review of 123 patients. Pediatrics 2003;111:715–21.

5 Coppock JS, Hardman JM, Bacon PA, Woods KL, Kendall MJ. Objective relief of vasospasm by glyceryl trinitrate in secondary Raynaud's phenomenon. Postgrad Med J 1986;62:8–15.

Rheumatology 2010;49:194–196
doi:10.1093/rheumatology/kep315
Advance Access publication 23 October 2009

A case of early-onset sarcoidosis with a six-base deletion in the *NOD2* gene

SIR, We present the first case of early-onset sarcoidosis (EOS, MIM no. 609464) with a six-base deletion in the *NOD2* gene, resulting in the replacement of one amino acid and the deletion of two additional amino acids. All previous mutations reported for EOS and Blau syndrome (BS, MIM no. 186580) were single-base substitutions that resulted in the replacement of a single amino acid [1–3].

The patient was a Japanese male born after an uncomplicated pregnancy and delivery. His family had no symptoms of skin lesions, arthritis or uveitis. At 5 years of age, he was diagnosed with bilateral severe uveitis. He became blind in both eyes during adolescence. He had swollen ankles without pain during childhood,

and developed arthritis in his both knees and ankles at 15 years of age. At 30 years, a skin rash had developed on his extremities after his first BCG vaccination. The skin lesions were scaly erythematous plaques with multiple lichenoid papules and some pigmentation. At the same age, camptodactyly without obvious synovial cysts of the hands was observed, and the deformity in all fingers developed by 35 years. At 41 years, he had low-grade fever for 1 year. He had no pulmonary lesions. His laboratory investigations showed normal white blood cell count, mildly elevated CRP (1.0 mg/dl) and ESR (20 mm/h). A skin biopsy from his left forearm revealed non-caseating granulomas without lymphocyte infiltration. There were no indications of infection by *Mycobacterium*.

The clinical symptoms and pathological findings on the biopsied skin indicated that the patient suffered from EOS. It has been reported that EOS and BS have a common genetic aetiology due to mutations in the *NOD2* gene that cause constitutive Nuclear Factor (NF)-κB activation [4, 5]. Thus we analysed the *NOD2* gene from the patient to look for mutations that might correlate with the pathology of EOS. A written informed consent was obtained from the patient and his families, according to the protocol of the institutional review board of Kyoto University Hospital and in accordance with the Declaration of Helsinki. Genomic sequencing analysis of the patient's *NOD2* gene showed the presence of a heterozygous deletion of six bases in exon 4, which resulted in c.1493_1498delAACTGT, p.E498V, 499–500del (Fig. 1A). The mutation was novel and was not identified in 100 normal controls. A genome alignment of *NOD2* among several species showed that E498, L499 and L500 are conserved from zebrafish to human (Fig. 1B). These data strongly suggested that the identified deletion of six bases in the *NOD2* gene is not a single nucleotide polymorphism (SNP), but is probably responsible for EOS in the patient.

Previous studies report that *NOD2* mutations causing EOS/BS show constitutive activation of NF-κB [6–8]. Therefore, we investigated the level of NF-κB activity associated with the new mutation identified here. First, we confirmed the level of mRNA expression of the mutated allele by subcloning analysis of *NOD2*-cDNA, which showed that the mutated allele was expressed as well as the wild type allele (data not shown). We then evaluated the ability of the *NOD2* mutant to constitutively activate NF-κB by using an *in vitro* reporter system in HEK293T cells transfected with both *NOD2* mutants and NF-κB reporter plasmids (Fig. 1C). The deletion mutant demonstrated almost five times more NF-κB activity than wild type without muramyl dipeptide (MDP) stimulation. Western blot analysis confirmed that NOD2 mutant protein expression was similar to that of wild type (Fig. 1C). Thus, like other mutations of *NOD2* identified previously, the deletion mutant identified here also showed constitutive activation of NF-κB.

The mechanism underlying EOS/BS has not been totally understood, although two pathways downstream from *NOD2* have been identified: NF-κB activation through receptor-interacting protein (RIP) like interacting caspase-like apoptosis regulatory protein kinase (RICK) and MAP kinase activation through the caspase recruitment domain 9 (CARD9) [9]. We previously tested 10 *NOD2* missense mutations that have been identified in our cohort of EOS/BS patients in Japan, and all of them demonstrated constitutive activation of NF-κB [3]. By analysing this newly identified deletion mutant, we have further confirmed the importance of constitutive activation of NF-κB by mutated *NOD2* for the pathogenesis of EOS/BS. We would like to emphasize the

FIG. 1 (**A**) Summary of the mutations identified in our patient. (**B**) NOD2 protein alignment among different species on the mutated amino acids. (**C**) NF-κB reporter assay using the *NOD2* deletion mutant. *In vitro* NF-κB reporter assays were performed as previously described [1, 3, 6, 7]. Mock vector, wild type *NOD2* (WT) and three *NOD2* variants (R334W, C495Y, H496L) derived from EOS/BS patients, were used as controls. Values represent the mean of normalized data (mock without MDP = 1) of triplicate cultures, and error bars indicate S.D. Shown is one representative result of three independent experiments. Protein expression levels of *NOD2* mutants analysed by western blotting are shown in the bottom panel.

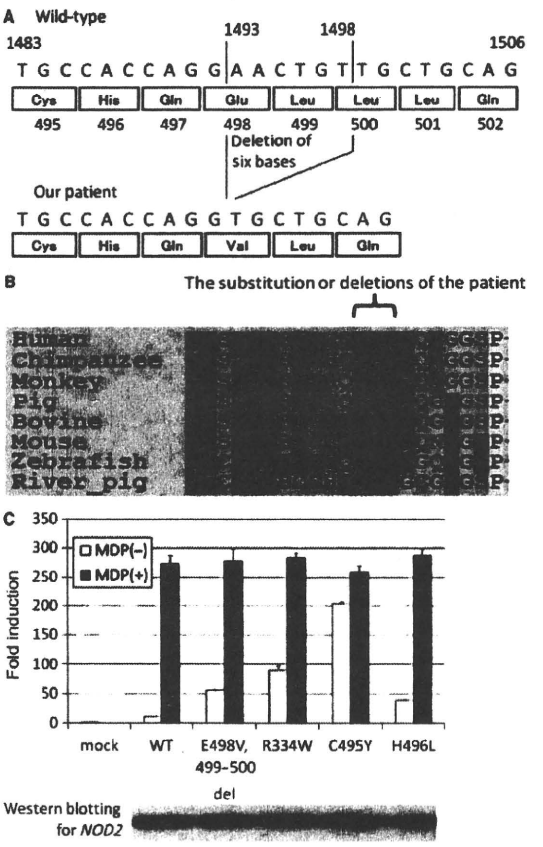

usefulness of the NF-κB reporter assay with mutant *NOD2* for observing its role in EOS/BS, although the MAP kinase activation pathway and other possible pathways need to be evaluated to more completely understand the pathogenesis of the *NOD2* mutation in EOS/BS.

We have identified the first deletion mutation in the *NOD2* gene responsible for EOS/BS, and the mutant showed constitutive activation of NF-κB, which is one of the key features that lead to the pathogenesis of EOS/BS.

Rheumatology key message

- A six-base deletion in *NOD2* gene causes EOS.

Acknowledgement

This work was carried out at Department of Pediatrics, Kyoto University Graduate School of Medicine, Kyoto, Japan.

Funding: This work was supported by grants from the Japanese Ministry of Education, Culture, Sports, Science and Technology and grants from the Japanese Ministry of Health, Labor and Welfare.

Disclosure statement: The authors have declared no conflicts of interest.

Hidemasa Sakai[1], Shusaku Ito[2], Ryuta Nishikomori[1], Yuuki Takaoka[1], Tomoki Kawai[1], Megumu Saito[1], Ikuo Okafuji[3], Takahiro Yasumi[1], Toshio Heike[1] and Tatsutoshi Nakahata[1]

[1]Department of Pediatrics, Kyoto University Graduate School of Medicine, Kyoto, [2]Department of Dermatology, Hitachi General Hospital, Hitachi and [3]Department of Pediatrics, Kobe City Medical Center General Hospital, Kobe, Japan
Accepted 27 August 2009
Correspondence to: Ryuta Nishikomori, Department of Pediatrics, Kyoto University Graduate School of Medicine, 54 Kawahara-cho, Shogoin, Sakyo-ku, Kyoto 606-8507, Japan. E-mail: rnishiko@kuhp.kyoto-u.ac.jp

References

1 Rosé CD, Wouters CH, Meiorin S *et al.* Pediatric granulomatous arthritis: an international registry. Arthritis Rheum 2006;54:3337–44.

2 Aróstegui JI, Arnal C, Merino R *et al. NOD2* gene-associated pediatric granulomatous arthritis: clinical diversity, novel and recurrent mutations, and evidence of clinical improvement with interleukin-1 blockade in a Spanish cohort. Arthritis Rheum 2007;56:3805–13.

3 Okafuji I, Nishikomori R, Kanazawa N *et al.* Role of the *NOD2* genotype in the clinical phenotype of Blau syndrome and Early-onset sarcoidosis. Arthritis Rheum 2009;60:242–50.

4 Kanazawa N, Okafuji I, Kambe N *et al.* Early-onset sarcoidosis and *CARD15* mutations with constitutive nuclear factor κB activation: common genetic etiology with Blau syndrome. Blood 2005;105:1195–97.

5 Rosé CD, Doyle TM, McIlvain-Simpson G *et al.* Blau syndrome mutation of *CARD15/NOD2* in sporadic early onset granulomatous arthritis. J Rheumatol 2005;32:373–5.

6 Chamaillard M, Philpott D, Girardin SE *et al.* Gene-environment interaction modulated by allelic heterogeneity in inflammatory diseases. Proc Natl Acad Sci USA 2003;100:3455–60.

7 Becker ML, Rosé CD. Blau syndrome and related genetic disorders causing childhood arthritis. Curr Rheumatol Rep 2005;7:427–33.

8 Kambe N, Nishikomori R, Kanazawa N. The cytosolic pattern-recognition receptor NOD2 and inflammatory granulomatous disorders. J Dermatol Sci 2005;39:71–80.

9 Hsu YM, Zhang Y, You Y *et al.* The adaptor protein CARD9 is required for innate immune responses to intracellular pathogens. Nat Immunol 2007;8:198–205.

Rheumatology 2010;49:196–197
doi:10.1093/rheumatology/kep330
Advance Access publication 25 October 2009

Comment on: Hepatotoxicity rates do not differ in patients with rheumatoid arthritis and psoriasis treated with methotrexate

Sir, We read with interest the recent article by Amital *et al.* [1] that compared hepatotoxicity rates in PsA and RA patients treated with MTX based on the evaluation of standard liver function tests. The authors conclude that the incidence of hepatotoxicity does not differ between the two disease groups after adjusting for the cumulative dose of MTX.

Several studies in MTX-treated psoriasis patients have reported that isolated abnormalities of liver enzymes (i.e. alkaline phosphatase, aspartate aminotransferase and alanine aminotransferase) were poor predictors of the severity of liver histopathology. The authors state that the combined sensitivity of aspartate aminotransferase, alanine aminotransferase and bilirubin for detecting an abnormal liver biopsy has been rated at 0.86 based on a previous study [2]. This figure implies that 14% of those with normal liver function tests will have undetected hepatic disease. Larger studies have suggested that 30–50% of the psoriasis patients on MTX have normal standard liver function test results despite histology showing fibrosis and cirrhosis [3]. The lack of correlation between liver enzymes and hepatic fibrosis and cirrhosis has been the major factor leading to the recommendation that liver biopsies be done to monitor potential hepatotoxicity. In this study, the liver function tests were performed with varying frequency which could allow abnormal liver function tests to be missed. The authors acknowledge that the rates of other hepatotoxic agents such as alcohol use and the occurrence of other hepatic comorbidities were not known. We believe that these are significant confounding variables, which make the interpretation of the results of this study difficult. The British Association of Dermatologists recommends serial monitoring

Pediatr Nephrol (2010) 25:545–548
DOI 10.1007/s00467-009-1370-z

BRIEF REPORT

A family with X-linked benign familial hematuria

Kazunari Kaneko · Sachiyo Tanaka · Masafumi Hasui · Kandai Nozu · Rafal Przybyslaw Krol · Kazumoto Iijima · Keisuke Sugimoto · Tsukasa Takemura

Received: 23 September 2009 / Revised: 19 October 2009 / Accepted: 22 October 2009 / Published online: 24 November 2009

Abstract Gene mutations in *COL4A5* located on Xq22 are believed to cause X-linked Alport syndrome, whereas mutations in *COL4A3* and *COL4A4* located on chromosome 2 are associated with autosomal inherited Alport syndrome or benign familial hematuria. A family with benign familial hematuria caused by *COL4A5* mutation, implying X-linked transmission, is reported here for the first time. This result suggests that *COL4A5* should be added to the list of causative genes for benign familial hematuria, although the mechanism(s) by which the same mutation leads to the distinct phenotypes, i.e. X-linked Alport syndrome or benign familial hematuria, remains unknown.

Keywords Alport syndrome · Benign familial hematuria · *COL4A5* gene

Introduction

Both Alport syndrome (AS) and benign familial hematuria (BFH) are inherited disorders associated with type IV collagen. However, these disorders are quite distinct clinically, with AS characterized by progressive nephritis with hematuria and proteinuria, sensorineural deafness, and ocular abnormalities, while BFH is characterized by prominent diffuse thinning of the glomerular basement membrane (GBM), lifelong glomerular hematuria, and normal renal function. Mutations in the *COL4A5* gene located on Xq22 are believed to cause X-linked AS (XLAS), whereas mutations in *COL4A3* and *COL4A4* genes located on chromosome 2 can be causes of the autosomal-recessive and autosomal-dominant type of AS or BFH [1–4]. The *COL4A5*, *COL4A3*, and *COL4A4* genes encode the alpha-5, alpha-3, and alpha-4 chains, respectively, of type IV collagen.

To the best of our knowledge, this is the first report of a family with BFH with a mutation in the *COL4A5* gene associated with aberrant expression of the alpha-5 chain in the skin and a mode of inheritance confirmed to be X-linked.

K. Kaneko (✉) · S. Tanaka · M. Hasui
Department of Pediatrics, Kansai Medical University,
2-3-1 Shin-machi,
Hirakata-shi, Osaka 573-1191, Japan
e-mail: kanekok@hirakata.kmu.ac.jp

K. Nozu · R. P. Krol · K. Iijima
Department of Pediatrics,
Kobe University Graduate School of Medicine,
Kobe, Japan

K. Sugimoto · T. Takemura
Department of Pediatrics, Kinki University School of Medicine,
Osaka, Japan

Methods

DNA sequencing

Genomic DNA was isolated from peripheral blood samples using standard phenol–chloroform extraction methods, as reported previously [5]. Briefly, primer pairs for each exon of *COL4A3*, *COL4A4*, and *COL4A5* were generated to amplify all exons, including the exon–intron boundaries of the genes. These PCR primers are listed elsewhere [5]. The PCR analysis and the direct sequence method were used to determine the DNA sequence with an automated DNA sequencer (model 310; Applied Biosystems, Foster City, CA).

Immunostaining of the skin

The methods are described in detail elsewhere [6]. Briefly, sections from frozen skin tissues, 3 μm thick, were used for immunofluorescent staining of type IV collagen. Double fluorochrome immunofluorescence staining for the alpha-5 and alpha-2 chains of type IV collagen was carried out using fluorochrome-conjugated monoclonal antibodies for AS (Shigei Medical Research Institute, Okayama, Japan).

Skin sections were reacted with fluorescein isothiocyanate-conjugated-anti-type IV collagen alpha-5 chain and Texas-Red-anti-type IV collagen alpha-2 chain and then observed under the immunofluorescent microscopy. Control sections were stained with nonimmune rat serum or an unrelated rat monoclonal antibody. These controls were entirely negative.

Case report

The index patient, a 9-year-old girl, was found to have hematuria through a mass screening program for renal diseases in Japan. She was referred to our hospital for further evaluation of persistent hematuria (3 years). The physical examination revealed no abnormalities, and she did not suffer from hypertension, sensorineural deafness, or eye involvement. Laboratory tests revealed only microscopic hematuria (erythrocytes >50/high power field, urinary protein 15 mg/dl). Values obtained in the hematological, biochemical, and serological tests were: serum creatinine:hemoglobin 12.3 g/dl, total protein 6.7 g/dl, uric acid 3.6 mg/dl, cholesterol 194 mg/dl, complement component 3 101 mg/dl, blood urea nitrogen 16 mg/dl, and creatinine 0.45 mg/dl.

The patient was born following a full-term normal pregnancy as the first child of unrelated Japanese parents. The family history was remarkable in that multiple family members had been diagnosed with BFH in her father's pedigree (Fig. 1). Her father, younger sister, paternal grandmother, paternal aunts, and paternal cousins have also been followed for hematuria by neighboring doctors since their childhood. Urinalyses and blood chemistries of these relatives disclosed isolated microscopic hematuria, but none had end-stage renal disease, sensorineural hearing loss, or eye complications such as lenticonus. It should be noted that even a male patient (her father, 38-year-old) demonstrated only trace occult blood, was negative for protein by the urine dipstick test, and was normotensive with normal serum biochemical markers including total protein (6.8 g/dl), blood urea nitrogen (12.8 mg/dl), and creatinine (0.89 mg/dl).

Although the clinical diagnosis of BFH was made based on these findings, the family's desire for a definitive diagnosis prompted us to perform skin biopsy to rule out the possibility of XLAS. The skin tissues obtained from the proband and her father revealed mosaic expression and a weak distribution of the alpha-5 chain of type IV collagen, respectively, in the epidermal basement membranes (Fig. 2), which are typically seen in a family with XLAS.

Although we recommended renal biopsy to the proband's father in order to distinguish between BFH and a mild phenotype of XLAS, he did not accept our proposal. We therefore performed an analysis of the genetic mutations of *COL4A3*, *COL4A4*, and *COL4A5* after obtaining informed consent. The results of sequence analysis of the *COL4A5* gene disclosed a heterozygous mutation for c.2999G>T in exon 34 (p.G1000V) in both the proband and her father; there were, however, no mutations in the *COL4A3* and *COL4A4* genes (Fig. 1). Further analyses of her kindred confirmed that only family members with hematuria (a younger sister and a paternal cousin) had the same mutation (Fig. 1). These mutations have not been described before nor have they been observed in 166 control chromosomes from healthy individuals.

Discussion

BFH is characterized by prominent diffuse thinning of the GBM on an ultrastructural level and lifelong glomerular hematuria that may be accompanied by mild proteinuria, normal renal function, and an autosomal-dominant inheritance pattern [1, 2]. It likely affects at least 1% of the general population [3].

AS is also an inherited disorder affecting the basement membranes. It is caused by mutations in genes encoding the alpha-3, alpha-4, and alpha-5 chains of type IV collagen. Transmission of AS can be X-linked, autosomal-recessive, or autosomal-dominant because these genes are located on chromosome 2 (COL4A3 and COL4A4, 2q35-37) and on the X chromosome (COL4A5, Xq26-48).

Our current state of knowledge links patients with homozygous or compound heterozygous *COL4A3* and *COL4A4* mutations to autosomal-recessive AS, while heterozygous carriers of mutations in these genes may account for up to 50% of patients with BFH [2, 7–10]. However, some families with BFH do not show any link to the COL4A3 or COL4A4 gene locus, suggesting that it is likely that other gene(s) may be responsible for similar phenotypes of BFH [2]. Slajpah et al. recently analyzed the mutations in genes for *COL4A3*, *COL4A4*, and *COL4A5* in Slovenian patients with AS or BFH [3]. Their results are of particular interest in that one missense mutation of *COL4A5* was found in six families, of which five appeared clinically to present with BFH [3]. Unfortunately, the protein expression of the alpha-5 chain of type IV collagen in a

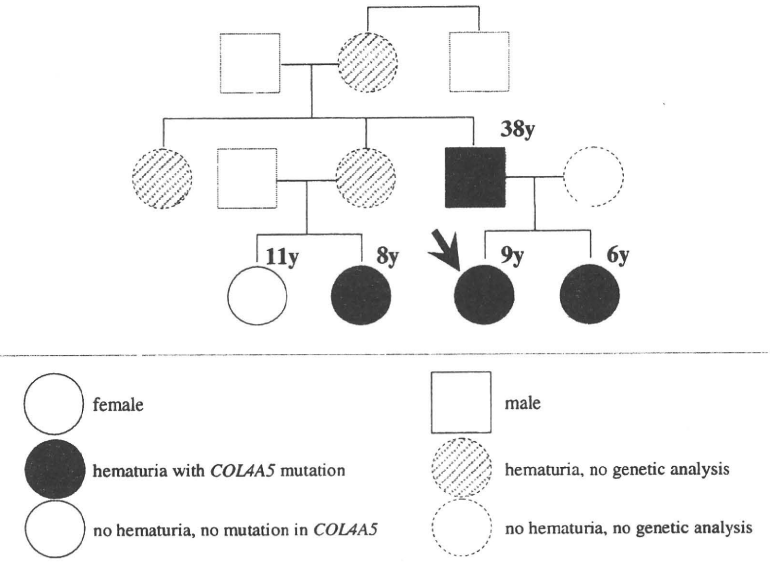

Fig. 1 Pedigree of the presenting family. Multiple family members have mutations in the *COL4A* genes and show asymptomatic isolated hematuria. *Arrow* Proband

biopsy specimen, such as skin or kidney tissue, was not described in these studies. Recent advances in diagnostic approaches for AS and BFH include immunohistochemical studies with monoclonal antibodies directed against the alpha chains using a specimen obtained from the skin because alpha chains of type IV collagen are normally located in the basement membranes of various tissues and organs, including the kidney, cochlea, eye, and skin [6, 11]. In the family presenting here, a mutation in *COL4A5*, which resulted in decreased or mosaic expression of alpha-5 chain in the epidermal basement membranes, seems to be associated with BFH.

To the best of our knowledge, this is the first report of a family with X-linked BFH.

In terms of genotype–phenotype correlations, the mechanism(s) determining that mutations in *COL4A5* lead to one of the distinct phenotypes, i.e., XLAS or BFH, remains obscure. Gross et al. focused on the different types of mutations and their locations on the *COL4A5* gene and classified XLAS into three types: (1) severe type caused by large rearrangements, premature stop, frameshift, donor splice site, and mutations involving the NC1-domain; (2) moderate–severe type caused by non-glycine XY-missense and glycine-XY mutations; (3) moderate type caused by

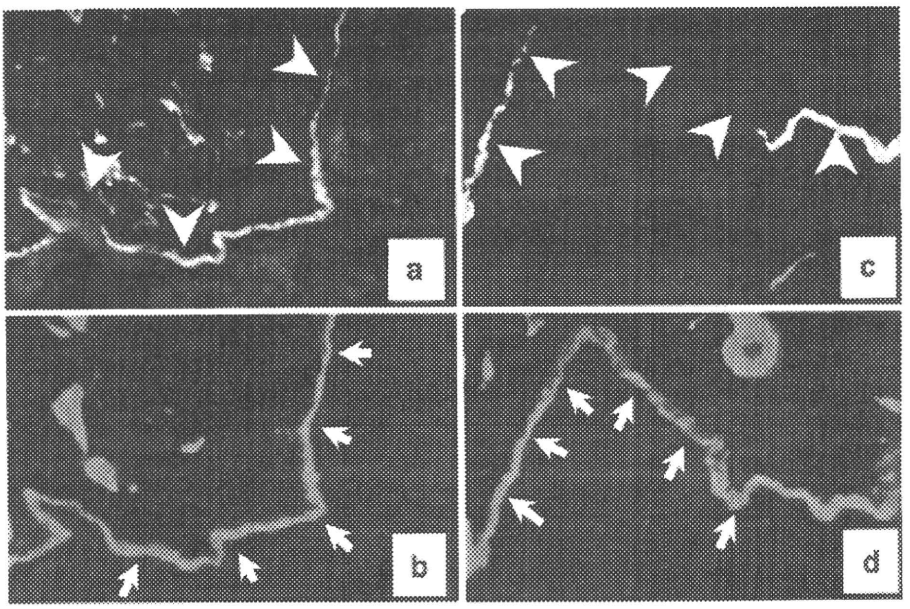

Fig. 2 Distribution of the alpha-2 and alpha-5 chains of type IV collagen in the epidermal basement membrane. Localization of the alpha-2 and alpha-5 chains was expressed as *red* and *green fluorescence*, respectively (indirect double label immunofluorescent technique, original magnification ×200). An alpha-5 chain was distributed diffusely but weakly in the membrane of the father (**a**, *arrowheads*) and as a mosaic pattern in the proband (**c**, *arrowheads*). An alpha-2 chain was stained in the normal linear pattern in both the father and the proband (**b**, **d**, *arrows*)

glycine-XY mutations [12]. Slajpah et al. also postulated that one missense mutation led to the glycine substitutions found in five unrelated families who clinically presented with BFH [3]. Thus, the glycine-XY missense mutation detected in our family has been reported to result in the mild phenotype, such as less severe forms of XLAS or BFH, and it could be speculated that XLAS and BFH may represent two opposite poles of the spectrum of hereditary *COL4A5* nephropathies [3].

Another possibility for the mild phenotype, despite a mutation in the *COL4A5* gene, may be somatic mosaicism. Two cases of somatic mosaicism have been reported recently [13, 14]. Direct nucleotide sequencing of the *COL4A5* gene in the DNA from the leukocytes and urine sediments of our young patient, however, identified only a single mutational peak (data not shown), while the patient with XLAS caused by somatic mosaicism [14] was reported to demonstrate two peaks—the mutant and the wild-type alleles of the *COL4A5* gene. Therefore, somatic mosaicism for a mutation of the *COL4A5* gene is unlikely in our presenting family.

In conclusion, we believe that *COL4A5* in addition to *COL4A3* or *COL4A4* should be added to the list of causative genes for BFH.

Acknowledgments This study was partly supported by the Mami Mizutani Foundation and Hyogo Prefecture Health Promotion Association.

Conflict of interest None to declare

References

1. Hudson BG, Tryggvason K, Sundaramoorthy M, Neilson EG (2003) Alport's syndrome, Goodpasture's syndrome, and type IV collagen. N Engl J Med 348:2543–2556
2. Pierides A, Voskarides K, Athanasiou Y, Ioannou K, Damianou L, Arsali M, Zavros M, Pierides M, Vargemezis V, Patsias C, Zouvani I, Elia A, Kyriacou K, Deltas C (2009) Clinico-pathological correlations in 127 patients in 11 large pedigrees, segregating one of three heterozygous mutations in the *COL4A3/COL4A4* genes associated with familial haematuria and significant late progression to proteinuria and chronic kidney disease from focal segmental glomerulosclerosis. Nephrol Dial Transplant 24:2721–2729
3. Slajpah M, Gorinsek B, Berginc G, Vizjak A, Ferluga D, Hvala A, Meglic A, Jaksa I, Furlan P, Gregoric A, Kaplan-Pavlovcic S, Ravnik-Glavac M, Glavac D (2007) Sixteen novel mutations identified in *COL4A3*, *COL4A4*, and *COL4A5* genes in Slovenian families with Alport syndrome and benign familial hematuria. Kidney Int 71:1287–1295
4. Knebelmann B, Breillat C, Forestier L, Arrondel C, Jacassier D, Giatras I, Drouot L, Deschênes G, Grünfeld JP, Broyer M, Gubler MC, Antignac C (1996) Spectrum of mutations in the COL4A5 collagen gene in X-linked Alport syndrome. Am J Hum Genet 59:1221–1232
5. Barker DF, Denison JC, Atkin CL, Gregory MC (2001) Efficient detection of Alport syndrome COL4A5 mutations with multiplex genomic PCR-SSCP. Am J Med Genet 98:148–160
6. Takemura T, Yanagida H, Yagi K, Moriwaki K, Okada M (2003) Alport syndrome and benign familial hematuria (thin basement membrane disease) in two brothers of a family with hematuria. Clin Nephrol 60:195–200
7. Lemmink HH, Nillesen WN, Mochizuki T, Schröder CH, Brunner HG, van Oost BA, Monnens LA, Smeets HJ (1996) Benign familial hematuria due to mutation of the type IV collagen α4 gene. J Clin Invest 98:1114–1118
8. Tryggvason K, Patrakka J (2006) Thin basement membrane nephropathy. J Am Soc Nephrol 17:813–822
9. Badenas C, Praga M, Tazón B, Heidet L, Arrondel C, Armengol A, Andrés A, Morales E, Camacho JA, Lens X, Dávila S, Milà M, Antignac C, Darnell A, Torra R (2002) Mutations in the *COL4A4* and *COL4A3* genes cause familial benign hematuria. J Am Soc Nephrol 13:1248–1254
10. Rana K, Tonna S, Wang YY, Sin L, Lin T, Shaw E, Mookerjee I, Savige J (2007) Nine novel *COL4A3* and *COL4A4* mutations and polymorphisms identified in inherited membrane diseases. Pediatr Nephrol 22:652–657
11. Patey-Mariaud de Serre N, Garfa M, Bessiéres B, Noël LH, Knebelmann B (2007) Collagen alpha5 and alpha2(IV) chain coexpression: analysis of skin biopsies of Alport patients. Kidney Int 72:512–516
12. Gross O, Netzer KO, Lambrecht R, Seibold S, Weber M (2002) Meta-analysis of genotype-phenotype correlation in X-linked Alport syndrome: impact on clinical counselling. Nephrol Dial Transplant 17:1218–1227
13. Plant KE, Boye E, Green PM, Vetrie D, Flinter FA (2000) Somatic mosaicism associated with a mild Alport syndrome phenotype. J Med Genet 37:238–239
14. Krol RP, Nozu K, Nakanishi K, Iijima K, Takeshima Y, Fu XJ, Nozu Y, Kaito H, Kanda K, Matsuo M, Yoshikawa N (2008) Somatic mosaicism for a mutation of the *COL4A5* gene is a cause of mild phenotype male Alport syndrome. Nephrol Dial Transplant 23:2525–2530

 DOI 10.1002/eji.200939886 Eur. J. Immunol. 2010. 40: 548–558

Galectin-9 expands immunosuppressive macrophages to ameliorate T-cell-mediated lung inflammation

Tomohiro Arikawa[*1], *Naoki Saita*[*2], *Souichi Oomizu*[1], *Masaki Ueno*[3], *Akihiro Matsukawa*[4], *Shigeki Katoh*[5], *Keisuke Kojima*[2], *Keiko Nagahara*[6], *Minoru Miyake*[6], *Akira Yamauchi*[5], *Hirotsugu Kohrogi*[2] *and Mitsuomi Hirashima*[1]

[1] Departments of Immunology and Immunopathology, Faculty of Medicine, Kagawa University, Kagawa, Japan
[2] Department of Respiratory Medicine, Faculty of Medical and Pharmaceutical Sciences, Kumamoto University, Kumamoto, Japan
[3] Departments of Inflammation Pathology, Faculty of Medicine, Kagawa University, Kagawa, Japan
[4] Department of Pathology and Experimental Medicine, Graduate School of Medicine, Dentistry and Pharmaceutical Sciences, Okayama University, Okayama, Japan
[5] Department of Cell Regulation, Faculty of Medicine, Kagawa University, Kagawa, Japan
[6] Department of Oral & Maxillofacial Surgery, Faculty of Medicine, Kagawa University, Kagawa, Japan

Galectin-9 (Gal-9) plays pivotal roles in the modulation of innate and adaptive immunity to suppress T-cell-mediated autoimmune models. However, it remains unclear if Gal-9 plays a suppressive role for T-cell function in non-autoimmune disease models. We assessed the effects of Gal-9 on experimental hypersensitivity pneumonitis induced by *Trichosporon asahii*. When Gal-9 was given subcutaneously to C57BL/6 mice at the time of challenge with *T. asahii*, it significantly suppressed *T. asahii*-induced lung inflammation, as the levels of IL-1, IL-6, IFN-γ, and IL-17 were significantly reduced in the BALF of Gal-9-treated mice. Moreover, co-culture of anti-CD3-stimulated CD4 T cells with BALF cells harvested from Gal-9-treated mice on day 1 resulted in diminished CD4 T-cell proliferation and decreased levels of IFN-γ and IL-17. $CD11b^+$ $Ly\text{-}6C^{high}F4/80^+$ BALF Mϕ expanded by Gal-9 were responsible for the suppression. We further found *in vitro* that Gal-9, only in the presence of *T. asahii*, expands $CD11b^+Ly\text{-}6C^{high}F4/80^+$ cells from BM cells, and the cells suppress T-cell proliferation and IFN-γ and IL-17 production. The present results indicate that Gal-9 expands immunosuppressive $CD11b^+Ly\text{-}6C^{high}$ Mϕ to ameliorate Th1/Th17 cell-mediated hypersensitivity pneumonitis.

Key words: Galectin-9 · Immune suppression · Lung · Macrophage · Pneumonitis

Introduction

Galectin-9 (Gal-9), a β-galactoside binding lectin, is a ligand for T-cell immunoglobulin- and mucin domain-containing molecule 3 (Tim-3), which plays crucial roles in innate and adaptive immunity *via* Gal-9/Tim-3 interactions [1, 2]. Tim-3 is expressed on terminally differentiated Th1 cells, Th17 cells and innate immune cells, such as DC [2–4]. Gal-9 induces apoptosis of activated Th1 and Th17 cells, in part, through the Ca^{2+}-calpain-caspase1 pathway [5], resulting in the amelioration of

Correspondence: Professor Mitsuomi Hirashima
e-mail: mitsuomi@kms.ac.jp

*These authors contributed equally to this work.

immunopathology in murine autoimmune disease models such as collagen-induced arthritis (CIA), autoimmune diabetes, and EAE [2, 6, 7]. Little is known, however, as to whether mechanisms other than apoptosis of Th1/Th17 cells are involved in Gal-9-mediated suppression of inflammation. We have shown, for example, that Gal-9 also enhances Treg generation from naïve $CD4^+$ T cells in a murine CIA model [7]. Although we have previously shown that Gal-9 induces DC maturation [8] and weakly promotes TNF-α production from DC [2], it has been widely accepted that certain types of Mϕ/DC, including myeloid-derived suppressor cells (MDSC) and regulatory DC (DCreg), also exhibit immunosuppressive function in a variety of immune responses [9–11]. Thus, the involvement of immunosuppressive Mϕ/DC also in Gal-9-mediated immune suppression cannot be excluded.

Exogenous particles, as well as autoantigens, are involved in the pathogenesis of T-cell-mediated inflammation. For example, hypersensitivity pneumonitis (HP), including Farmer's lung and summer-type HP, is a T-cell-mediated inflammation caused by inhalation of particles, bacteria, *etc.* [12, 13]. Repeated inhalation of organic dust can cause HP, which is characterized by inflammatory lung disease with alveolitis and granuloma formation [13]. Hyperactive pro-inflammatory Th1 cells are closely associated with the etiology of HP [14]. It is thus important to assess whether Gal-9 might be involved in T-cell-mediated inflammation other than that associated with autoimmune diseases.

The purpose of the study presented here is to show whether Gal-9 attenuates the severity of murine experimental HP characterized by Th1 and Th17 cell-mediated inflammation. We show that Gal-9 expands $CD11b^+Ly\text{-}6C^{high}$ Mϕ that exhibit immunosuppression of T-cell proliferation and activation, thereby ameliorating Th1/Th17 cell-mediated HP.

Results

Effect of Gal-9 on experimental HP

Preliminary experiments to assess the dose effects of subcutaneously injecting Gal-9 (0.3, 3, and 30 μg/mouse) revealed that 3 μg/mouse of Gal-9 was sufficient to ameliorate experimental HP, although 0.3 μg/mouse was not. Therefore, 3 μg/mouse of Gal-9 was used for further experiments.

Significant weight loss was not observed during the course of experimental HP. Histological analyses on day 7 post-challenge with *Trichosporon asahii* revealed a marked infiltration of inflammatory cells, consisting mainly of mononuclear cells, in alveolar septal, peribronchial, and perivascular areas in PBS-treated mice (Fig. 1A). The histological scores for Gal-9-treated mice (1.68 ± 0.09, $n = 10$) were significantly lower than those for PBS-treated mice (2.83 ± 0.05, $n = 10$), indicating that Gal-9 exerted a suppressive effect on experimental HP (Fig. 1A). The numbers of BALF cells from both groups of mice were counted. Total BALF cell numbers were similar in both groups until day 3 post-challenge (Fig. 1B). Gal-9 treatment resulted in a significant decrease in total cell number on day 7 post-challenge. The numbers of specific inflammatory cell types, including Mϕ, PMN, and lymphocytes, were also counted using Giemsa staining. Infiltrated Mϕ exhibited kinetics similar to those of the total cells until day 3, while Gal-9 treatment decreased the number of PMN only in the early phase of experimental HP (6 h to day 1). Increased lymphocyte accumulation was detected in the BALF of PBS-treated mice from days 3 to 7, but this was markedly suppressed by Gal-9 treatment. BALF was obtained from each group on day 7 post-challenge to determine the concentrations of several cytokines by ELISA. As expected, Gal-9 treatment significantly decreased the levels of the pro-inflammatory cytokines IL-1β and IL-6 (Fig. 1C). Gal-9 also significantly suppressed the levels of Th1-related IL-12p40, IFN-γ and Th17-related IL-17 cytokines. IL-13 and IL-4 levels were under the detection limits in this model (data not shown). The proportions of Tim-3, but not Tim-1, expressing $CD4^+$ T cells in BALF cells on day 7 were significantly decreased by Gal-9 treatment (Fig. 2A). On the other hand, Gal-9 up-regulated the proportion of $CD4^+$ $CD25^+Foxp3^+$ Treg in spleen on days 3 and 7 but not on day 1 (Fig. 2B), indicating that Gal-9 exerts its effect in experimental HP at least partly in its late phase by reducing the number of Tim-3-expressing Th1 and Th17 cells, and by increasing Treg as previously shown [7].

Inhibition of T-cell proliferation by BALF cells obtained from Gal-9 treated mice

To identify the phenotypes of infiltrated cells from Gal-9-treated mice, flow cytometric analysis was performed on day 1 post-challenge. Subsequently, we assessed whether BALF cells from Gal-9-treated mice had suppressive effects on T-cell functions. BALF cells from Gal-9-treated mice were co-cultured with CD3 Ab-stimulated $CD4^+$ T cells *in vitro*. BALF cells obtained from Gal-9-treated mice on day 1 post-challenge significantly inhibited $CD4^+$ T-cell proliferation in a dose-dependent manner (Fig. 3A). To further ascertain the influence of BALF cells from Gal-9-treated mice on $CD4^+$ T-cell cytokine production, intracellular staining for IFN-γ was carried out for stimulated-$CD4^+$ T cells *in vitro*. Co-culture with BALF cells from Gal-9-treated mice nearly completely suppressed IFN-γ production by $CD4^+$ T cells, as compared to $CD4^+$ T cells co-cultured with BALF cells from PBS-treated mice (Fig. 3B). Thus, it appeared likely that BALF cells from Gal-9 treated mice have suppressive effects on both the proliferation and function of $CD4^+$ T cells. These suppressive effects, however, were not observed for BALF cells obtained from Gal-9-treated mice on day 7 (data not shown). In addition, cytokine concentrations were determined in the culture supernatants. The concentrations of IFN-γ, IL-2, IL-17, and IL-4, but not IL-10, were significantly decreased by co-culturing $CD4^+$ T cells with BALF cells from Gal-9-treated mice (Fig. 3C) though the amounts of TNF-α and IL-6 were only minimally decreased (data not shown).

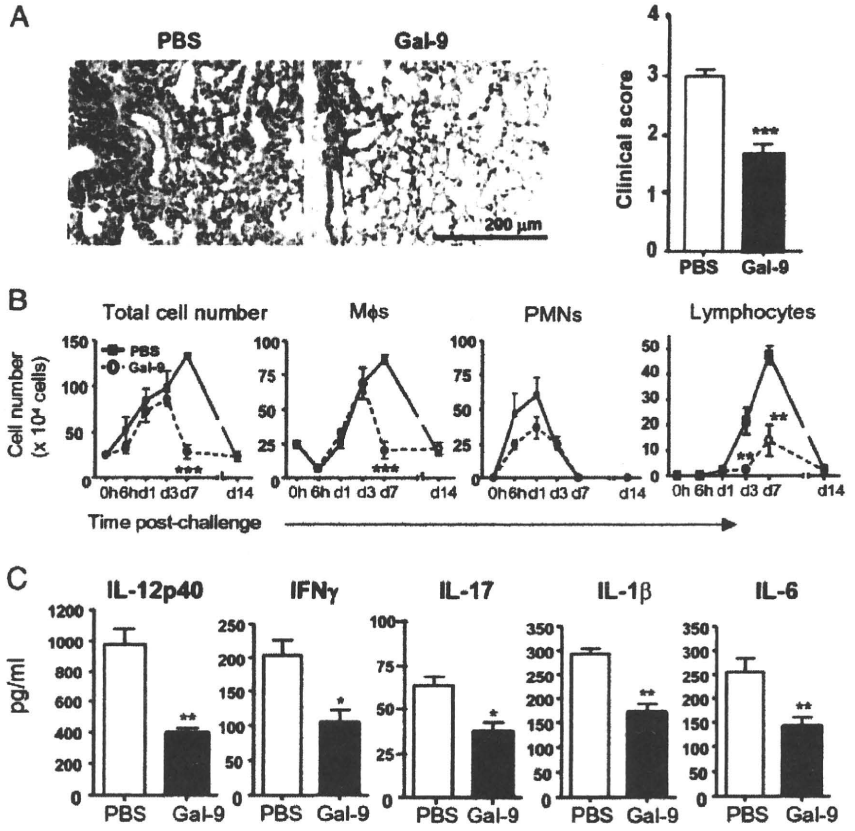

Figure 1. Effect of Gal-9 on experimental HP. Mice were treated with *T. asahii*. Lungs were harvested on day 7 post-challenge as described in the *Materials and methods* section. (A) Each photomicrographs represents one of ten separate experiments. H & E Staining; scale bar = 200 μm. The degree of inflammation (clinical score) was evaluated by the relative percentages of inflammatory cells infiltrating the lung as described in the *Materials and methods* section. Results are mean+SEM, with ten animals in each group. ***$p<0.001$ compared with control group. (B) The kinetics of immune cells in BALF from Gal-9-treated and PBS-treated mice. The numbers of total cells, Mϕ, PMN, and lymphocytes were counted at the indicated times post-challenge using Diff Quick kit staining. **$p<0.01$, ***$p<0.001$ compared with control group. (C) Effects of Gal-9 on cytokine production in inflamed lungs. BALF obtained from each group on day 7 post-challenge was assayed by ELISA. **$p<0.01$, ***$p<0.001$ compared with control group. Significance was evaluated by a non-parametric two-tailed Mann–Whitney *U*-test and by two-way ANOVA.

Expansion of immunosuppressive CD11b$^+$Ly-6C$^+$ Mϕ by Gal-9

Despite decreased infiltration of PMN into the lung as described above (Fig. 1B), Gal-9-treatment significantly increased CD11b$^+$ Gr-1$^+$ cells in BALF (16.73%±2.91; $p<0.01$) compared with their levels in PBS-treated mice (4.98%±1.36) on day 1 post-challenge. Since recent studies revealed that Gr-1 exhibits cross reactivity with Ly-6G and Ly-6C [15], specific antibodies against Ly-6G and Ly-6C Ag were used to identify which cell types are responsible for the suppressive activity of BALF cells from Gal-9-treated mice. The phenotypic differences of infiltrated immune cells in the BALF cells from PBS- and Gal-9-treated mice on days were 1, 3, and 7 post-challenge by flow cytometry. The frequency of CD11b$^+$Ly-6C^{high} cells was significantly increased in BALF on day 1 post-challenge as compared with their levels in PBS-treated mice, and this increase was sustained until day 3 (Fig. 4A and B). On the other hand, the frequency of CD11b$^+$Ly-6G^{high} cells was decreased in BALF on day 1 post-challenge (Fig. 4A). Further morphological analysis revealed that CD11b$^+$Ly-6C$^-$Ly-6G^{high} cells were mostly mature PMN, whereas CD11b$^+$Ly-6C^{high}Ly-6G$^-$ cells were larger, monocyte/Mϕ-like mononuclear cells with round or reniform nuclei and a vacuolated cytoplasm (Fig. 4C). We also asked whether Gal-9 affects systemic myelo-monocytic differentiation in this model. Expansion of CD11b$^+$Ly-6C^{high} (Gr-1^{int}) cells was detected in the spleen of Gal-9-treated HP mice on days 1, 3, and 7 post-challenge (data not shown). Ly-6C^{high} cells in BALF cells were next depleted in order to characterize the suppressive role of CD11b$^+$Ly-6C^{high} cells that were increased by Gal-9-treatment. Ly-6C^{high} cell-depleted BALF cells failed to suppress T-cell proliferation, although BALF cells suppressed proliferation before the Ly-6C^{high} cell depletion (Fig. 4D).

CD11b$^+$Ly-6C^{high}Ly-6G cells were further found to co-express F4/80, but they did not express CD86 or CD80 (Fig. 5A). In contrast, expression of PDCA-1, CD11c, and B220 was weakly detected in CD11b$^+$Ly-6C^{high}Ly-6G cells. Furthermore, 81.1%±3.5 ($n=3$) of the Gal-9-expanded CD11b$^+$Ly-6C$^+$ Ly-6G$^-$ cells were CD16/32$^+$ cells, whereas the level of CD14$^+$

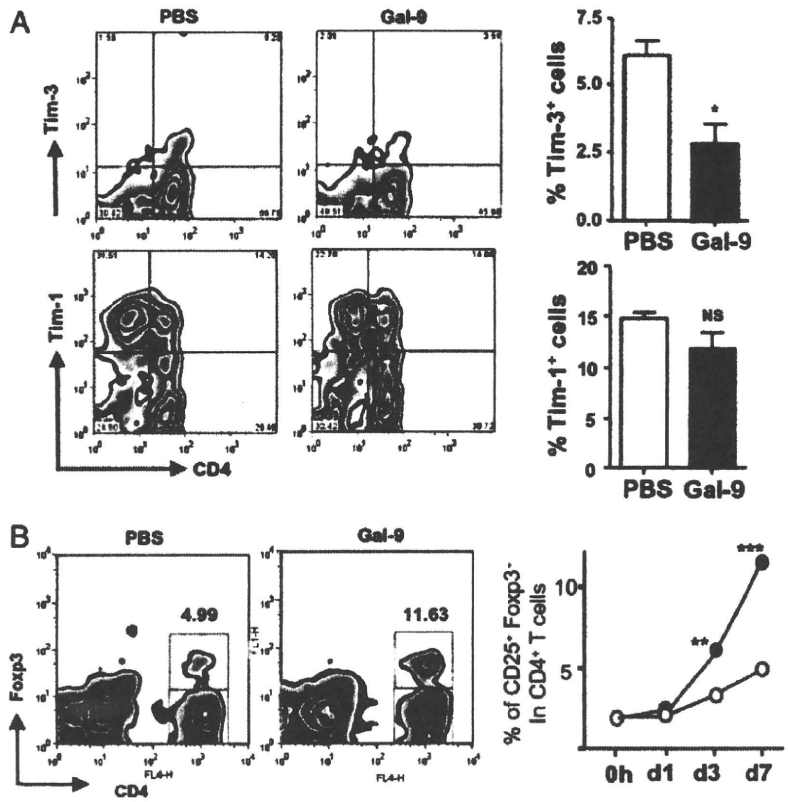

Figure 2. Proportion of Tim3-expressing CD4 T cells and $CD4^+CD25^+Foxp3^+$ Treg in experimental HP mice. (A) $CD4^+$ Tim-3^+ cells and $CD4^+$ Tim-1^+ cells in BALF cells obtained on day 7 post-challenge were analyzed by flow cytometry. A representative result showing 1 of 3 independent experiments is shown. Data are represented as the mean+SEM. NS, not significant, $^*p<0.05$ compared with the control group. (B) Gal-9 up-regulated Treg in spleen on day 3 to day 7 as compared to PBS control cells. A representative result for one of three independent experiments is shown. Significance was evaluated by non-parametric two-tailed Mann–Whitney *U*-test. $^{**}p<0.01$, $^{***}p<0.001$ compared with the control group.

cells was negligible, suggesting that Gal-9-expanded $CD11b^+$Ly-$6C^+$Ly-$6G^-$ cells are "immature" macrophage-lineage cells.

Arginase 1 and iNOS expression was also assessed in $F4/80^+$ cells in BALF by Western blot. $F4/80^+$ cells in BALF from Gal-9-treated mice had high arginase 1 expression compared with PBS-treated mice (Fig. 5B). In contrast, expression of iNOS was not detected in either PBS- or Gal-9-treated mice. Immunohistological analyses confirmed that $F4/80^+$ cells from Gal-9-treated mice had much higher arginase 1 immunoreactivity in their cytoplasms (Fig. 5C). Quantitative assays further indicated that there was a significantly higher percentage of arginase 1^+ cells in $F4/80^+$ cells in BALF from Gal-9-treated mice than in BALF from PBS-treated mice (Fig. 5D).

Gal-9 induces maturation of BM cells to $CD11b^+$ Ly-$6C^{high}$ Mϕ *in vitro*

Our present results suggested that Gal-9 expands a $CD11b^+$ $Ly6C^{high}$ cell population in this experimental HP model. We thus designed experiments to assess the effects of Gal-9 on the differentiation of BM cells to $CD11b^+$ cells expressing Ly-6C *in vitro*. BM cells were prepared from naïve mice and cultured with Gal-9 in the presence or absence of *T. asahii* for 5 days. Gal-9 alone increased the proportion of $CD11b^+Ly6C^-$ Mϕ, but *T. asahii* minimally increased the proportion of $CD11b^+Ly6C^{high}$ Mϕ. When BM cells were cultured with Gal-9 and *T. asahii*, the proportion of $CD11b^+Ly6C^{high}$ Mϕ was significantly increased (Fig. 6A and B), while Ly-6G expression was not affected by Gal-9 and/or *T. asahii* (Fig. 6A). Taken together, these results indicate that both Gal-9 and *T. asahii* are required for significant expansion of $CD11b^+Ly6C^{high}$ Mϕ from BM cells.

Effects of BM cell-derived $CD11b^+Ly6C^{high}$ Mϕ generated by Gal-9 and *T. asahii* on T-cell proliferation

We performed experiments to determine whether $CD11b^+$ $Ly6C^{high}$ Mϕ induced by Gal-9 and *T. asahii* also suppress $CD4^+$ T-cell proliferation. The $CD11b^+Ly6C^{high}$ Mϕ (G1 in Fig. 7A), $CD11b^+Ly6C^{int}$ Mϕ (G2) or $CD11b^+Ly6C^-$ Mϕ (G3) were sorted and then co-cultured with $CD4^+$ T cells in anti-CD3/CD28 Ab-coated plates for 3 days. The $CD11b^+Ly6C^{high}$ Mϕ almost completely suppressed $CD4^+$ T-cell proliferation, while

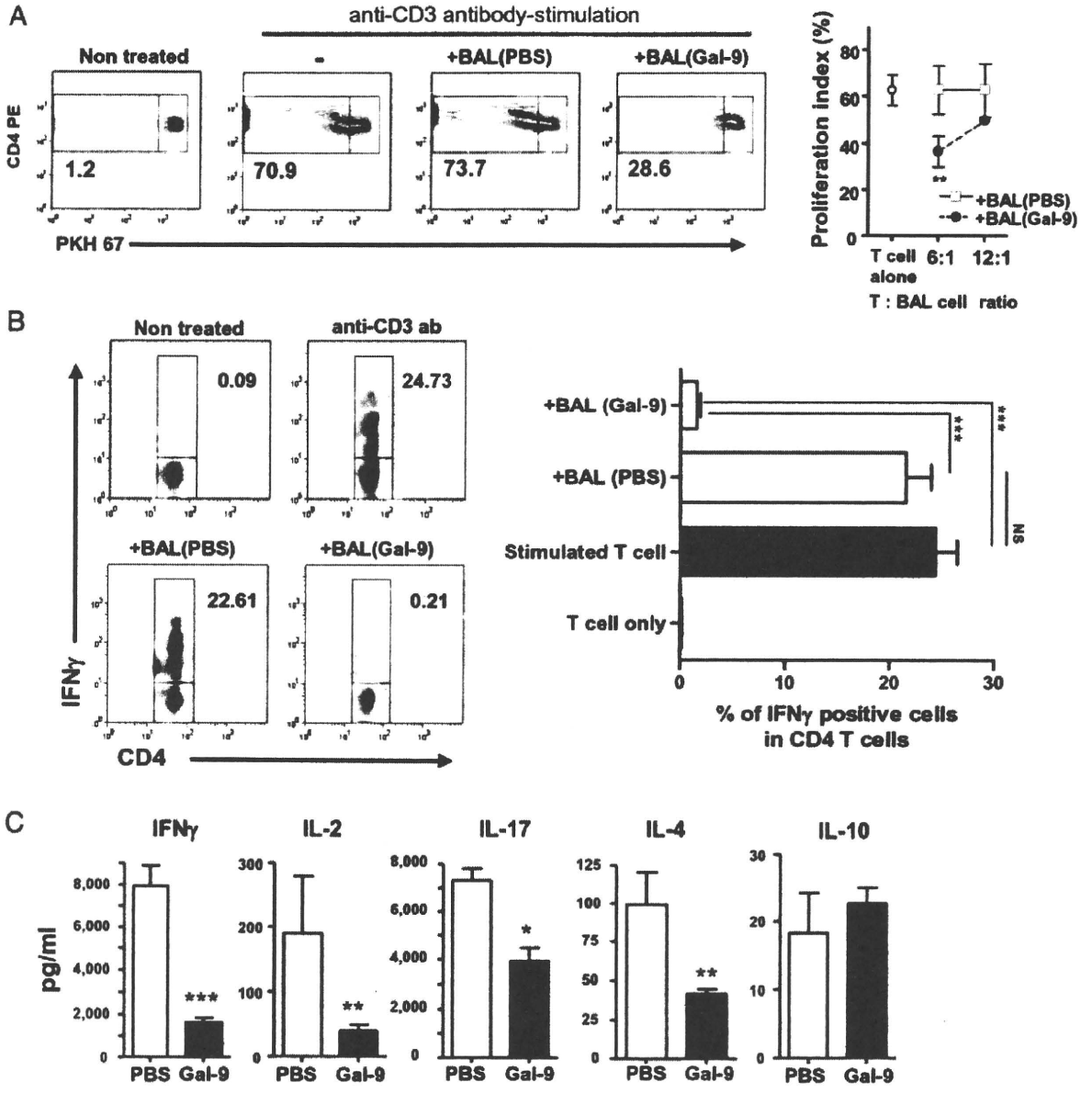

Figure 3. Functional analysis of BALF cells from Gal-9-treated experimental HP mice. (A) BALF cells from Gal-9-treated mice suppress T-cell proliferation. $CD4^+$ T cells were harvested from spleens of PBS-treated mice and stained with PKH 67. BALF cells obtained on day 1 post-challenge were cocultured with PKH67 pre-stained $CD4^+$ T cells. Cells were analyzed by flow cytometry after 3 days in culture. Results are mean ± SEM, with 6 animals in each group. Filled circles: BALF cells from Gal-9-treated mice, open squares: BALF cells from PBS-treated mice. $^{**}p < 0.01$ compared with control group. (B) Gal-9 treatment decreases IFN-γ production by $CD4^+$ T cells. Splenic $CD4^+$ T cells and BALF cells from experimental HP mice were co-cultured for 3 days with or without CD3 stimulation. Harvested cells were stained with the indicated fluorochrome-labeled antibodies and analyzed by flow cytometry. Results are mean+SEM. NS, not significant; $^{***}p<0.001$ compared with control group. (C) Cytokines in culture supernatants from (B). Results are means of triplicates+SEM. $^{*}p<0.05$, $^{**}p<0.01$, $^{***}p<0.001$ compared with control group. Significance was evaluated by a non-parametric two-tailed Mann–Whitney *U*-test.

the $CD11b^+Ly6C^-$ Mϕ did not (Fig. 7B). $CD11b^+Ly6C^{int}$ Mϕ also exhibited suppressive activity on T-cell proliferation, although this activity was significantly weaker than that of $CD11b^+Ly6C^{high}$ Mϕ. Furthermore, IFN-γ and IL-17 levels from the stimulated $CD4^+$ T cells were decreased by co-culture with $CD11b^+Ly6C^{high}$ Mϕ (Fig. 7C). In contrast to IFN-γ and IL-17, IL-4 levels were negligible in all cases (data not shown).

Discussion

HP is a pulmonary hypersensitivity reaction characterized by a massive lymphocyte infiltration into the lungs [12]. It has been shown that T cells, especially Th1 cells, play a pivotal role in the pathogenesis of HP as indicated by increased levels of IFN-γ and IL-12 in the lung [14, 16]. In addition to a Th1/Th2 imbalance,

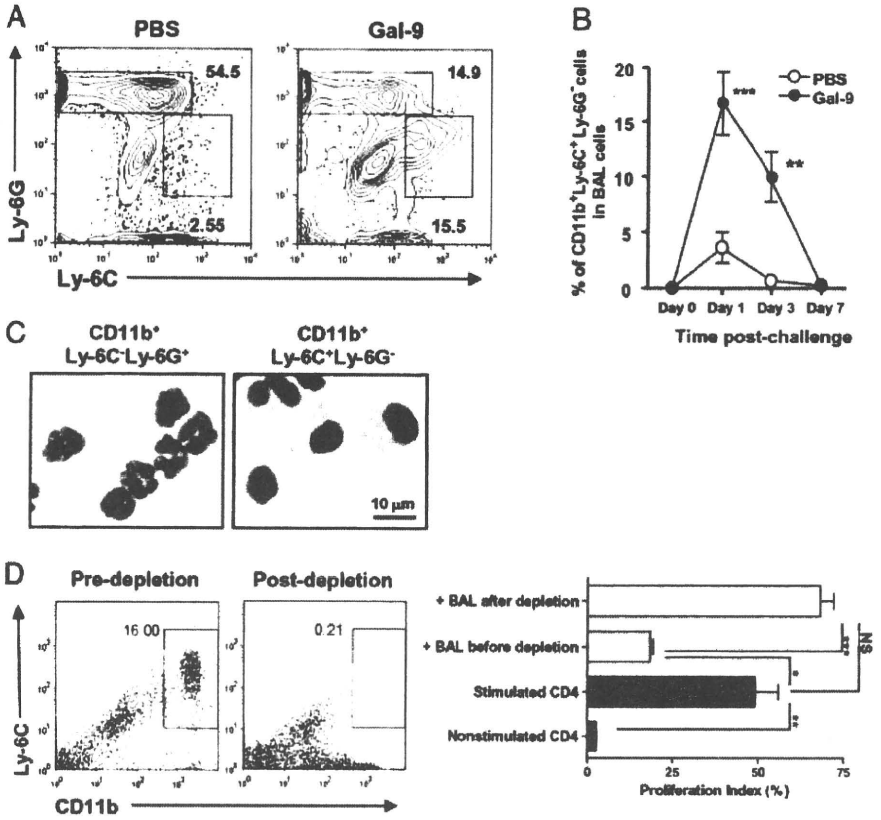

Figure 4. Morphological and functional analyses of Gal-9-expanded CD11b$^+$Ly-6C$^+$ cells. (A) BALF cells from Gal-9-treated mice and PBS-treated mice were stained with CD11b, Ly-6C and Ly-6G. Representative results on day 1 for 1 of 3 independent experiments. (B) Kinetics of CD11b$^+$Ly-6C$^+$ cells in BALF cells from each group on days 0, 1, 3, and 7 post-challenge. Results are means ± SEM, with six animals in each group. $^{**}p<0.01$, $^{***}p<0.001$ compared with control group. (C) Morphological analysis of CD11b$^+$Ly-6C-Ly-6G$^+$ cells and CD11b$^+$Ly-6C$^+$Ly-6G cells. Cells were sorted as described in the *Materials and methods* section and then stained with Giemsa stain. Bar = 10 μm. (D) The effects of CD11b$^+$Ly-6C$^+$ cell depletion on T-cell proliferation. BALF cells were obtained from Gal-9-treated mice, and Ly-6C$^+$ cells were depleted by specific Ly-6C Ab and rabbit complement system as described in the *Materials and methods* section. Next, Ly-6C depleted or non-depleted BALF cells were co-cultured with CD4 T cells during anti-CD3/CD28 stimulation (BALF cells:CD4 T cell, 1:2). Results are means of triplicates + SEM. NS, not significant, $^{*}p<0.05$, $^{**}p<0.01$, $^{***}p<0.001$ compared with control group. Significance was evaluated by a non-parametric two-tailed Mann–Whitney U-test.

insufficient Treg function appears critical for the pathogenesis of HP, as blockade of co-stimulatory signals using CTLA4-Ig administration reduced pulmonary inflammation by decreasing specific auto-antibody and cytokine production [17]. Previous results have shown that Gal-9 may induce apoptosis of Tim-3-expressing Th1 cells *via* Gal-9/Tim-3 interaction [1], and that Gal-9 induces the up-regulation of Treg [7]. Furthermore, highly pro-inflammatory IL-17-producing Th17 cells also express Tim-3 on their surfaces [3]. In fact, Gal-9 was found to decrease the number of Tim-3-expressing CD4 T cells and increase the number of CD4$^+$CD25$^+$Foxp-3$^+$ Treg on days 3 and 7 of experimental HP, raising the hypothesis that Gal-9 suppresses experimental HP, at least in part, by the above mechanisms in the late phase of experimental HP.

Our results indicate that Gal-9 treatment suppressed experimental HP *in vivo*, based on the levels of IFN-γ and IL-17 in the BALF and on the clinical scores on day 1 post-challenge relative to PBS-challenged controls. Intriguingly, co-culture of T cells with BALF cells from Gal-9-treated mice on day 1 post-challenge suppressed T-cell proliferation and IFN-γ production after CD3 stimulation *in vitro*. We further found that CD11b$^+$Ly-6C^{high} F4/80$^+$ cells with monocyte/Mϕ morphology may be responsible for this suppression.

It is well known that expansion of MDSC occurs in cancer patients and in tumor-bearing mice, and that these MDSC negatively affect T-cell expansion and effector functions [9–11]. Expansion of MDSC has also been induced after exposures to bacterial [18], parasitic [19–21] and viral Ag [22], and after traumatic stress [23]. Recent studies have also shown that MDSC are a group of myeloid cells comprised of precursors of macrophages, granulocytes, DC, and myeloid cells at earlier stages of differentiation [11, 23]. Monocytic MDSC express CD11b, Gr-1 and F4/80, but low levels of markers for mature APC, including CD80, CD86 and others [24, 25]. This suggests that MDSC are mainly immature Mϕ-lineage cells, although granulocytic MDSC are also involved in immune suppression in tumor-bearing mice [22]. A previous report by Augusto *et al.* has shown that monocytic MDSC in patients with metastatic renal cell carcinoma

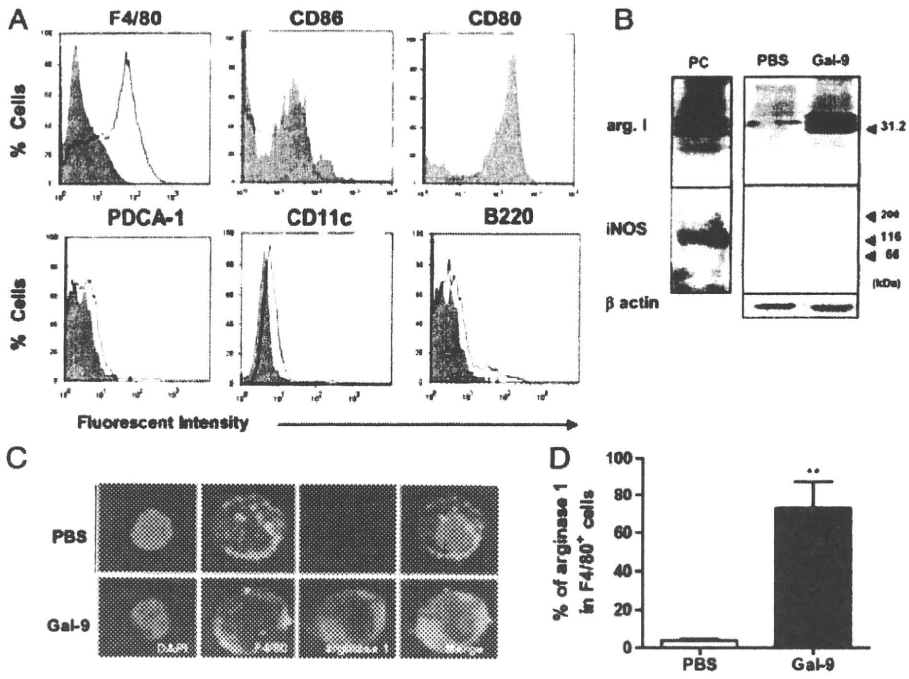

Figure 5. Phenotypes of CD11b$^+$Ly-6C$^+$Ly-6G$^-$ cells. (A) BALF cells from Gal-9-treated mice on day 1 post-challenge were stained with CD11b, Ly-6C, and several cell-surface markers as shown in the figure. Panels show several charts in the CD11b$^+$Ly-6C$^+$ gated region. Line histograms show expression of the respective Ag, and filled histograms show the respective controls. Results are representative of three independent experiments. (B) Western blot analysis for arginase 1 and iNOS. Cell extracts of F4/80$^+$BALF cells from each group were used. Extracts of mouse liver and whole lung tissue were used as positive controls for NOS2 and arginase 1, respectively. One representative blot showing results of three experiments is shown. PC, positive control. (C) Immunofluorescence assay of BALF cells. DAPI (blue), F4/80-positive cells (Green), arginase 1 positive cells (red); merged photographs are shown. Representative data from one of four experiments are shown. (D) Percentage of arginase 1$^+$ cells in F4/80$^+$ cells as shown in (C). More than 300 F4/80$^+$ cells were observed, and then the percentage of arginase 1$^+$ cells was calculated. $^{**}p<0.01$ compared with the control group. Significance was evaluated by a non-parametric two-tailed Mann–Whitney *U*-test.

express CD11b but not CD14 [26]. Our experiments showed that CD16/32 is expressed in Gal-9-expanded CD11b$^+$Ly-6C$^+$Ly-6G cells, whereas expression of CD14, CD80, and CD86 is negligible in those cells, suggesting that Gal-9-expanded CD11b$^+$Ly-6C$^+$ Ly-6G$^-$ cells are "immature" macrophages with MDSC activity (monocytic MDSC).

Recent studies have shown that MDSC (CD11b$^+$Ly-6C$^+$ Ly-6G$^-$ cells) use arginase 1 and/or iNOS to regulate T-cell function by inducing cell death or inhibiting proliferation [9, 10, 23]. Accumulated evidence has revealed that induction of arginase 1 in MDSC involves IL4/IL-13/IL-10/TGF-β/*etc.*, while induction of iNOS involves IFN-γ/*etc.* [11, 23, 27]. The present results indicate there is more arginase 1 but not iNOS protein in the lysates of BAL cells from Gal-9-treated mice, compared to PBS-treated mice. This raises the hypothesis that CD11b$^+$ Ly-6C^{high}Ly-6G cells expanded by Gal-9 in the lungs are affected by IL-4/TGF-β/IL-10 but not by IFN-γ because Gal-9 strongly suppresses IFN-γ production from terminally differentiated Tim-3$^+$ Th1 cells by inducing apoptosis [1, 7]. Furthermore, Gal-9 with or without *T. asahii* does not directly induce the induction of arginase 1 in BAL cells *in vitro* (data not shown), although CD11b$^+$Ly-6C^{high} cells expanded by Gal-9 with *T. asahii* exhibit evident immunosuppressive activity when they are co-cultured with T cells. This confirms the critical role of cytokines, such as IL-4/IL-13/IL-10/TGF-β, derived from co-cultured T cells in the induction of arginase 1.

We have shown that DC express Tim-3, and Gal-9/Tim-3 interaction activates DC to produce a small amount of TNF-α [2]. In contrast to DC, little or no Tim-3 expression has been detected in Mϕ [2]. The present experiments also indicate that CD11b$^+$ Ly-6C^{high}F4/80$^+$ cells expanded by Gal-9 express little Tim-3 on their surface (data not shown), suggesting little involvement of Gal-9/Tim-3 interaction in the expansion of CD11b$^+$Ly-6C^{high} F4/80$^+$ cells, though this remains to be established.

It has been shown that another type of cell, DCreg, also play a role in suppressing acute graft *versus* host disease [28], allergic airway inflammation [29] and acute lethal systemic inflammation [30]. DCreg have different phenotypic characteristics from the CD11b$^+$Ly-6C^{high}F4/80$^+$ cells; they strongly express CD11c and IA/I-E, and they have weak CD40, CD80, and CD86 expression [24]. Nobumoto *et al.* have previously shown that Gal-9 expands plasmacytoid DC (pDC)-like Mϕ that enhance NK activity in a tumor-bearing mouse model [31]. The CD11b$^+$Ly-6C^{high}Ly-6G cells in the present experiments probably differ from the pDC-like Mϕ, especially in the expression of CD11c, CD80, CD86, and PDCA-1. Gal-9 induces maturation of BM-derived hematopoietic precursors to CD11b$^+$Ly-6C^{high} cells only in the presence of *T. asahii*. Recently, it has been shown that MyD88-deficient mice

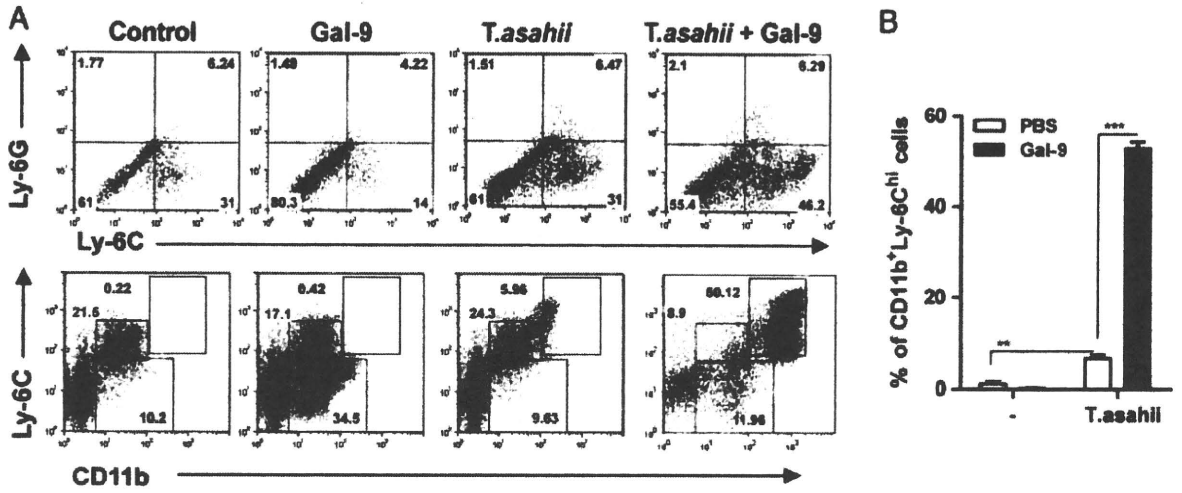

Figure 6. Gal-9 induces $CD11b^+Ly\text{-}6C^+$ cells, but not $Ly\text{-}6G^+$ cells, concomitant with *T. asahii* stimulation *in vitro*. (A) Enriched c-kit ($CD117^+$) positive cells from naive mice were cultured for 5 days in medium with or without *T. asahii* and in the presence or absence of Gal-9. FACS analysis was performed for each culture condition. The charts of Ly-6G and Ly-6C expression cells in $CD11b^+$ cells (top) and that of CD11b and Ly-6C expression cells (bottom) in each culture condition are shown. Representative results of three independent experiments. (B) Percentages of $CD11b^+$ $Ly\text{-}6C^+$ cells in A. Results are means of triplicates+SEM. $^{**}p<0.01$, $^{***}p<0.001$ compared with control group. Significance was evaluated by a non-parametric two-tailed Mann–Whitney *U*-test.

develop severe intestinal inflammation, indicating that MyD88 signaling plays an important protective role. This raises the possibility that Gal-9 up-regulates the immunosuppressive $CD11b^+$ $Ly\text{-}6C^{high}$ Mϕ or pDC-like Mϕ differently depending on the pathogenic circumstances (*T. asahii versus* tumor), because *T. asahii* appears to activate MyD88 through TLR on those cells.

Collectively, the studies presented here indicate that infiltration of $CD11b^+Ly\text{-}6C^{high}$ Mϕ, probably MDSC, into the lung at the early phase of experimental HP suppresses the severity of experimental HP. In addition, Gal-9 expands $CD11b^+Ly\text{-}6C^{high}$ Mϕ with suppressive activity on Th cell functions in BM cells.

Materials and methods

Animals

Female C57BL/6 mice (7–8 weeks old) were obtained from Charles River Laboratories Japan (Yokohama, Japan). Animals were kept in accordance with international guidelines and national law. The protocol of this study was approved by the Kagawa University Animal Care and Use Committee.

Expression and purification of recombinant stable Gal-9

Expression and purification of recombinant human stable Gal-9 was described previously [32, 33]. All Gal-9 preparations used in this report were >95% pure by SDS-PAGE with less than 0.3 endotoxin units/mL (<0.03 ng/mL), as assessed by a limulus turbimetric kinetic assay using a Toxinometer ET-2000 (Wako, Osaka, Japan). Protein concentration was determined with a bicinchoninic acid assay reagent (Pierce, Rockford, IL, USA), using BSA as a standard.

Ag

Particulate *T. asahii*, an etiologic agent of HP, was prepared as previously described [34]. The powdered material was suspended in sterile PBS (pH 7.4) at a concentration of 4 mg/mL and stored at −20°C until use.

Induction of HP

Mice were intranasally sensitized with 50 μL (200 μg/mouse) of *T. asahii* Ag three times daily. After 14 days, mice were challenged once with 50 μL (200 μg/mouse) of the Ag. Mice were simultaneously given either recombinant Gal-9 (0.3, 3, and 30 μg/mouse) or PBS subcutaneously. Differential cell counts for each mouse used Diff Quik staining (Baxter, McGaw Park, IL, USA) or Giemsa staining.

Histological studies

Sections of left lungs were stained with hematoxylin and eosin. Histological scores were graded from 0 to 4 as described previously [35]; 0: no inflammatory cells, 1: <10%, 2: 10–25%, 3: 25–50%, and 4: >50%.

Cytokine assays for BALF and culture supernatants

IL-2, TNF-α, IL-12p40, IFN-γ, IL-17, IL-1β, IL-4, IL-6, and IL-13 contents in BALF and culture supernatants were assayed by

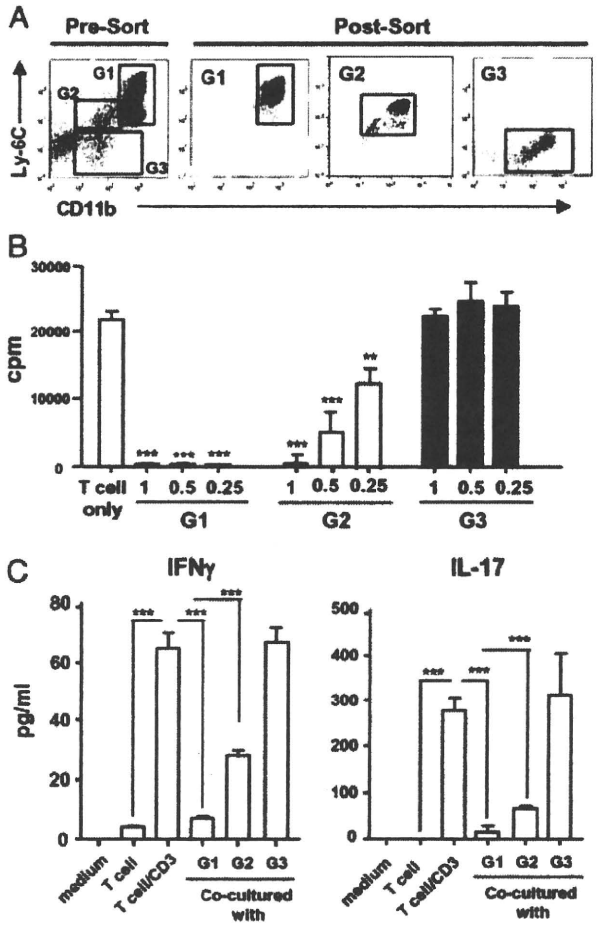

Figure 7. CD11b$^+$Ly-6C^{high} cells differentiated by Gal-9 *in vitro* have suppressive effects on CD4$^+$ T-cell proliferation. (A) CD11b$^+$Ly-6C^{high} cells significantly suppress CD4$^+$ T-cell proliferation. CD11b$^+$Ly-6C^{high}, CD11b$^+$Ly-6C^{int}, and CD11b$^+$Ly-6C$^-$ cells were sorted with a FACS Aria. G1, G2, and G3 represent isolated fractions of CD11b$^+$Ly-6C^{high} cells, CD11b$^+$Ly-6C^{low} cells, and CD11b$^+$Ly-6C$^-$ cells, respectively. Purities of cell fractions were >95%. (B) Following isolation of BM-derived cells after culture in medium containing *T. asahii* and Gal-9, CD4$^+$ T cells were cocultured with each cell type and stimulated in anti CD3/CD28 Ab-coated plates at varying ratios as shown in the figure. After 3 days of culture, [^{3}H] thymidine-uptake was evaluated. Results are means of triplicates+SEM. $^{**}p<0.01$, $^{***}p<0.001$ compared with control group. (C) IFN-γ and IL-17 levels in the culture supernatants from B were determined by ELISA. Results are means of triplicates+SEM. Significance was evaluated by a non-parametric two-tailed Mann–Whitney *U* test. $^{***}p<0.001$ compared with control group.

quantitative ELISA for murine cytokines/chemokines using cytokine-specific kits (R&D Systems, Minneapolis, MN, USA) as described previously [7].

Flow cytometry

BALF cells obtained from mice were washed in PBS with 0.5% FBS and incubated with appropriate fluorochrome-labeled antibodies, then analyzed by flow cytometry using a Becton Dickinson FACSCalibur (Becton Dickinson, San Jose, CA, USA). The following antibodies were used: anti-mouse Gr-1-FITC (eBioscience, San Diego, CA, USA), anti-mouse CD11b-PE (eBioscience), anti CD11b APC (Biolegend, San Diego, CA, USA), anti Ly-6C-FITC or PE (BD Pharmingen, San Jose, CA, USA), anti Ly-6G-PE (BD Pharmingen), anti-CD86-PE (Biolegend), anti CD80-FITC (eBioscience), anti-mouse IFN-γ-FITC (Biolegend), anti-mouse Tim-3-PE (eBioscience), anti-mouse Tim-1-PE (eBioscience), anti-Foxp3-APC (Biolegend), anti-mouse CD4-PE (eBioscience), anti-mouse PDCA-1-PE (eBioscience), CD11c-PE (eBioscience), anti-mouse CD14-PE (BD Pharmingen), anti-mouse CD16/32-PE (Biolegend), and anti-mouse B220-PE (eBioscience). Data were analyzed with FlowJo software (Tree Star, Ashland, OR, USA).

Immunohistochemical staining of BALF cells

BALF cells were placed on glass slides by cytospin (Cytospin 3, SHANDON, Waltham, MA, USA). After air-drying for 20 min, slides were fixed with 1% PFA/PBS for 10 min. After washing with 0.1% Tween-20/PBS, slides were blocked with 3% BSA/0.1% Tween-20/PBS for 1 h at room temperature, then incubated with polyclonal rabbit anti-mouse arginase 1 Ab (Santa Cruz) and Rat anti-mouse F4/80 Ab (AbD Serotec, Oxford, UK) at 4°C overnight, followed by incubation with Alexa Fluor 594-conjugated anti-rabbit Ab (Molecular Probes) and Alexa Fluor 488-conjugated anti-rat Ab (Molecular Probes, Japan, K.K. Tokyo, Japan), respectively. Fluorescent images were observed by confocal microscopy (Bio-Rad Radiance 2100, Bio-Rad). We observed more than 300 F4/80$^+$ cells and then calculated the percentage of arginase 1$^+$ cells in the F4/80$^+$ cells.

In vitro expansion of CD11b$^+$ Ly-6C$^+$ F4/80$^+$ cells

BM cells obtained from naïve female C57BL/6 mice were used for *in vitro* assays. BM cells were harvested from femurs and tibias, treated with RBC lysis solution, and then sorted for CD117$^+$ cells using a c-kit isolation kit (Miltenyi Biotec, Bergisch Gladbach, Germany) according to the manufacturer's protocol. The purity of CD117$^+$ cells was>60% in our experiments. Harvested cells were cultured with Gal-9 (3 and 30 nM) in the presence or absence of *T. asahii* for 5 days.

Cell sorting

Very stringent gating conditions were used for sorting experiments (FACSAria, Becton Dickinson), with purity checked by flow cytometry: CD11b$^+$Ly-6C$^+$Ly-6G$^-$ cells and CD11b$^+$Ly-6C$^-$ Ly-6G$^+$ cells were>95%.

Western blot

Harvested cell pellets were dissolved in SDS lysis buffer, boiled, fractionated on an SDS-polyacrylamide gel, and transferred to a nitrocellulose membrane. After blocking with PBS plus 0.1% Tween-20 containing 5% skim milk for 1 h at room temperature, the membrane was incubated with antibodies against NOS2 (Abcam, Cambridge, MA, USA) and arginase1 (Santa Cruz, CA, USA) overnight at 4°C. After washing with PBS plus 0.1% Tween-20, the membrane was incubated with anti-HRP-linked Ab for 1 h at room temperature and visualized with Western lightning chemiluminescence reagent (PerkinElmer, Waltham, MA, USA) according to the manufacturer's protocol. Extracts from mouse liver and whole lung tissue were used as positive controls for NOS2 and arginase 1, respectively.

Evaluation of suppressive effects on T-cell proliferation

T-cell proliferation was evaluated using splenic $CD4^+$ T cells and BALF cells obtained from PBS-treated mice or Gal-9-treated mice. In some experiments, Ly-$6C^+$ cells were depleted from BALF cells of Gal-9-treated mice using specific antibodies and rabbit complement system *in vitro* as described previously [36]. Generally, spleen cells were obtained at the time of BALF collection from experimental HP mice. $CD4^+$ T-cell purification and staining with PKH67 were performed according to the manufacturer's protocol (Sigma). Pre-stained $CD4^+$ T cells were diluted (BALF cells: T cells) 1:6 or 1:12, then co-cultured for 3 days. A T-cell proliferation index was evaluated by measuring the decreasing PKH67 staining intensities in $CD4^+$ T cells after co-culture with BALF cells.

For *in vitro* experiments, the effects of $CD11b^+$Ly-$6C^{high}$ or $CD11b^+$Ly-$6C^-$ cells on T-cell proliferation were assessed using [^{3}H] thymidine as described previously [11]. In brief, U-bottom 96-well plates were coated with anti-CD3/CD28 antibodies (1 μg/mL each) overnight at 4°C. $CD4^+$ T cells (0.3×10^5 cells/well) were purified using specific MACS beads (Miltenyi Biotec) and then cultured with plate-bound anti-CD3/CD28 for 3 days. The activated $CD4^+$ T cells were co-cultured with BM cell-derived $CD11b^+$Ly-$6C^{high}$, $CD11b^+$Ly-$6C^{int}$, and $CD11b^+$ Ly-$6C^-$ cells from the beginning of the culture. During the final 16 h of the 3-day culture, 1 μCi [^{3}H] thymidine was added, and the cells were then harvested. The supernatants (50 μL) were harvested before addition of [^{3}H] thymidine to measure cytokine levels.

Statistical analysis

For statistical comparisons, non-parametric two-tailed Mann–Whitney *U*-tests and two-way ANOVA were used. All statistical analyses were performed with Prism 4 software (GraphPad Software, La Jolla, CA, USA).

Acknowledgements: We thank Ms. Masako Seki, Ms. Kanako Ito, Ms. Megumi Nagayama and Mr. Tetsuya Shiota (GalPharma, Japan) for technical assistances and Dr. Aya Yokota (Faculty of Pharmaceutical Sciences at Kagawa Campus, Tokushima Bunri University, Japan) for technical assistance with cell sorting. This work was supported, in part, by a Grant-In-Aid for young scientists (B) 2008-2009 (20790570) to T. A. from the Japan Society for Promotion of Science (JSPS), by Kagawa University Characteristic Prior Research Fund 2009 to M. H., and by grants from the Japanese Ministry of Education, Culture, Sports, Science, and Technology.

Conflict of interest: The authors declare no financial or commercial conflict of interest.

References

1 **Zhu, C., Anderson, A. C., Schubart, A., Xiong, H., Imitola, J., Khoury, S. J., Zheng, X. X. *et al.***, The Tim-3 ligand galectin-9 negatively regulates T helper type 1 immunity. *Nat. Immunol.* 2005. **6**: 1245–1252.

2 **Anderson, A. C., Anderson, D. E., Bregoli, L., Hastings, W. D., Kassam, N., Lei, C., Chandwaskar, R. *et al.***, Promotion of tissue inflammation by the immune receptor Tim-3 expressed on innate immune cells. *Science* 2007. **318**: 1141–1143.

3 **Nakae, S., Iwakura, Y., Suto, H. and Galli, S. J.**, Phenotypic differences between Th1 and Th17 cells and negative regulation of Th1 cell differentiation by IL-17. *J. Leukoc. Biol.* 2007. **81**: 1258–1268.

4 **Monney, L., Sabatos, A. C., Gaglia, J. L., Ryu, A., Waldner, H., Chernova, T., Manning, S. *et al.***, Th1-specific cell surface protein Tim-3 regulates macrophage activation and severity of an autoimmune disease. *Nature* 2002. **415**: 536–541.

5 **Kashio, Y., Nakamura, K., Abedin, M. J., Seki, M., Nishi, N., Yoshida, N., Nakamura, T. and Hirashima, M.**, Galectin-9 induces apoptosis through the calcium-calpain-caspase-1 pathway. *J. Immunol.* 2003. **170**: 3631–3636.

6 **Chou, F. C., Shieh, S. J. and Sytwu, H. K.**, Attenuation of Th1 response through galectin-9 and T-cell Ig mucin-3 interaction inhibits autoimmune diabetes in NOD mice. *Eur. J. Immunol.* 2009. **39**: 2403–2411.

7 **Seki, M., Oomizu, S., Sakata, K-M., Sakata, A., Arikawa, T., Watanabe, K., Ito, K. *et al.***, Galectin-9 suppresses the generation of Th17, promotes the induction of regulatory T cells, and regulates experimental autoimmune arthritis. *Clin. Immunol.* 2008. **127**: 78–88.

8 **Dai, S. Y., Nakagawa, R., Itoh, A., Murakami, H., Kashio, Y., Abe, H., Katoh, S. *et al.***, Galectin-9 induces maturation of human monocyte-derived dendritic cells. *J. Immunol.* 2005. **175**: 2974–2981.

9 **Huang, B., Pan, P. Y., Li, Q., Sato, A. I., Levy, D. E., Bromberg, J., Divino, C. M. and Chen, S.H.**, Gr-$1^+$$CD115^+$ immature myeloid suppressor cells mediate the development of tumor-induced T regulatory cells and T-cell anergy in tumor-bearing host. *Cancer Res.* 2006. **66**: 1123–1131.

10 **Marhaba, R., Vitacolonna, M., Hildebrand, D., Baniyash, M., Freyschmidt-Paul, P. and Zöller, M .**, The importance of myeloid suppressor cells in the regulation of autoimmune effector cells by a chronic contact eczema. *J. Immunol.* 2007. **179**: 5071–5081.

11 **Youn, J.-I., Nagaraj, S., Collazo, M. and Gabrilovich, D. I.**, Subsets of myeloid-derived suppressor cells in tumor-bearing mice. *J. Immunol.* 2008. **181**: 5791–5802.

12 **Trentin, L., Migone, N., Zambello, R., Francia di Celle, P., Aina, F., Feruglio, C., Bulian, P. et al.**, Mechanisms accounting for lymphocytic alveolitis in hypersensitivity pneumonitis. *J. Immunol.* 1990. **145**: 2147–2154.

13 **Nance, S., Cross, R., Yi, A. K. and Fitzpatrick, E. A.**, IFN-γ production by innate immune cells is sufficient for development of hypersensitivity pneumonitis. *Eur. J. Immunol.* 2005. **35**: 1928–1938.

14 **Gudmundsson, G. and Hunninghake, G. W.**, Interferon-gamma is necessary for the expression of hypersensitivity pneumonitis. *J. Clin. Invest.* 1997. **99**: 2386–2390.

15 **Movahedi, K., Guilliams, M., Van den Bossche, J., Van den Bergh, R., Gysemans, C., Beschin, A., De Baetselier, P. and Van Ginderachter, J. A.**, Identification of discrete tumor-induced myeloid-derived suppressor cell subpopulations with distinct T cell-suppressive activity. *Blood* 2008. 111: 4233–4244.

16 **Gudmundsson, G., Monick, M. M. and Hunninghake, G. W.**, IL-12 modulates expression of hypersensitivity pneumonitis. *J. Immunol.* 1998. **161**: 991–999.

17 **Israel-Assayag, E., Fournier, M. and Cormier, Y.**, Blockade of T cell costimulation by CTLA4-Ig inhibits lung inflammation in murine hypersensitivity pneumonitis. *J. Immunol.* 1999. **163**: 6794–6799.

18 **Dalton, D. K., Haynes, L., Chu, C. Q., Swain, S. L. and Wittmer, S.**, Interferon eliminates responding CD4 T Cells during Mycobacterial Infection by inducing apoptosis of activated CD4 T Cells. *J. Exp. Med.* 2000. **192**: 117–122.

19 **Terrazas, L. I., Walsh, K. L., Piskorska, D., McGuire, E. and HarnJr, D. A.**, The schistosome oligosaccharide lacto-*N*-neotetraose expands Ly-6G$^+$ cells that secrete anti-inflammatory cytokines and inhibit proliferation of naive CD4$^+$ cells: a potential mechanism for immune polarization in helminth infections. *J. Immunol.* 2001. **167**: 5294–5303.

20 **Goni, O., Alcaide, P. and Fresno, M.**, Immunosuppression during acute *Trypanosoma cruzi* infection: involvement of Ly6G (Ly-6G(+)) CD11b(+)immature myeloid suppressor cells. *Int. Immunol.* 2002. **14**: 1125–1134.

21 **Bronte, V.**, Myeloid-derived suppressor cells in inflammation: Uncovering cell subsets with enhanced immunosuppressive functions. *Eur. J. Immunol.* 2009. **39**: 2670–2672.

22 **Melani, C., Sangaletti, S., Barazzetta, F. M., Werb, Z. and Colombo, M. P.**, Amino-biphosphonate-mediated MMP-9 inhibition breaks the tumor-bone marrow axis responsible for myeloid suppressor cell expansion and macrophage infiltration in tumor stroma. *Cancer Res.* 2007. **67**: 11438–11446.

23 **Makarenkova, V. P., Bansal, V., Matta, B. M., Perez, L. A. and Ochoa, J. B.**, CD11b$^+$/Ly-6G$^+$ myeloid suppressor cells cause T cell dysfunction after traumatic stress. *J. Immunol.* 2006. **176**: 2085–2094.

24 **Mazzoni, A., Bronte, V., Visintin, A., Spitzer, J. H., Apolloni, E., Serafini, P., Zanovello, P. and Segal, D. M.**, Myeloid suppressor lines inhibit T cell responses by an NO-dependent mechanism. *J. Immunol.* 2002. **168**: 689–695.

25 **Greifenberg, V., Ribechini, E., Rößner, S. and Lutz, M. B.**, Myeloid-derived suppressor cell activation by combined LPS and IFN-gamma treatment impairs DC development. *Eur. J. Immunol.* 2009. **39**: 2865–2876.

26 **Augusto, C. O, Arnold, H. Z., Claudia, H. and Rodrigues, P. C.**, Arginase, prostaglandins, and myeloid-derived suppressor cells in renal cell cartinoma. *Clin. Cancer Res.* 2007. **13**: 721–726.

27 **Sica, A. and Bronte, V.**, Altered macrophage differentiation and immune dysfunction in tumor development. *J. Clin. Invest.* 2007. **117**: 1155–1166.

28 **Sato, K., Yamashita, N., Yamashita, N., Baba, M. and Matsuyama, T.**, Regulatory dendritic cells protect mice from murine acute graft-versus-host disease and leukemia relapse. *Immunity.* 2003. **18**: 367–379.

29 **Fujita, S., Yamashita, N., Ishii, Y., Sato, Y., Sato, K., Eizumi, K., Fukaya, T. et al.**, Regulatory dendritic cells protect against allergic airway inflammation in a murine asthmatic model. *J. Allergy Clin. Immunol.* 2008. **121**: 95–104.

30 **Fujita, S., Seino, K., Sato, K., Sato, Y., Eizumi, K., Yamashita, N., Taniguchi, M. and Sato, K .**, Regulatory dendritic cells act as regulators of acute lethal systemic inflammatory response. *Blood* 2006. **107**: 3656–3664.

31 **Nobumoto, A., Oomizu, S., Arikawa, T., Katoh, S., Nagahara, K., Miyake, M., Nishi, N. et al.**, Galectin-9 expands unique macrophages exhibiting plasmacytoid dendritic cell-like phenotypes that activate NK cells in tumor-bearing mice. *Clin. Immunol.* 2009. **130**; 322–330.

32 **Nishi, N., Itoh, A., Fujiyama, A., Yoshida, N., Araya, S., Hirashima, M., Shoji, H. and Nakamura, T.**, Development of highly stable galectins: truncation of the linker peptide confers protease-resistance on tandem-repeat type galectins. *FEBS Lett.* 2005. **579**: 2058–2064.

33 **Matsushita, N., Nishi, N., Seki, M., Matsumoto, R., Kuwabara, I., Liu, F. T., Hata, Y. et al.**, Requirement of divalent galactoside-binding activity of ecalectin/galectin-9 for eosinophil chemoattraction. *J. Biol. Chem.* 2000. **275**: 8355–8360.

34 **Saita, N., Ando, M., Araki, S. and Yoshinaga, M.**, Fibroblast proliferation factors in pulmonary granuloma induced by *Trichosporon cutaneum* in rabbits: presence of a lymphocyte-derived fibroblast proliferation factor and its functional specificity. *Int. Arch. Allergy Appl. Immunol.* 1991. **95**: 294–302.

35 **Blanchet, M. R., Israël-Assayag, E. and Cormier, Y.**, Inhibitory effect of nicotine on experimental hypersensitivity pneumonitis *in vivo* and *in vitro*. *Am. J. Respir. Crit. Care Med.* 2004. **169**: 903–909.

36 **Nagahara, K., Arikawa, T., Oomizu, S., Kontani, K., Tateno, H., Watanabe, K., Niki, T. et al.**, Galectin-9 increases Tim-3$^+$dendritic cells and CD8$^+$ T cells and enhances antitumor immunity via galectin-9/Tim-3 interaction. *J. Immunol.* 2008. **118**: 7660–7669.

Abbreviations: **CIA:** collagen-induced arthritis · **DCreg:** regulatory DC · **Gal-9:** galectin-9 · **HP:** hypersensitivity pneumonitis · **MDSC:** myeloid-derived suppressor cell · **pDC:** plasmacytoid DC · **Tim-3:** T-cell immunoglobulin- and mucin domain-containing molecule 3

Full correspondence: Professor Mitsuomi Hirashima, Department of Immunology and Immunopathology, Faculty of Medicine, Kagawa University, 1750-1 Ikenobe, Miki-Cho, Kita-Gun, Kagawa 761-0793, Japan
Fax: +87-891-2119
e-mail: mitsuomi@kms.ac.jp

Received: 10/8/2009
Revised: 8/10/2009
Accepted: 23/10/2009